# The CRP-like transcriptional regulator MrpC curbs c-di-GMP and 3', 3' cGAMP nucleotide levels during development in *Myxococcus xanthus*

Sofya Kuzmich[1], Patrick Blumenkamp[2], Doreen Meier[3], Alexander Goesmann[2], Anke Becker[3] and Lotte Søgaard-Andersen[1#]

[1] Department of Ecophysiology, Max Planck Institute for Terrestrial Microbiology, Karl-von-Frisch Str. 10, 35043 Marburg, Germany

[2] Systems Biology and Bioinformatics, Justus Liebig University Giessen, Heinrich-Buff-Ring Str. 58, 35392 Gießen, Germany

[3] Center for Synthetic Microbiology (SYNMIKRO), Philipps Universität Marburg Karl-von-Frisch-Str. 14, 35043 Marburg, Germany

[#]Corresponding author
Tel. +49-6421-178 201
Fax +49-6421-178 209
E-mail: sogaard@mpi-marburg.mpg.de

**Running Title:** MrpC regulates c-di-GMP and cGAMP levels during development

**Keywords:** c-di-GMP, cGAMP, CRP, Cappable-seq, sporulation, fruiting body formation, development, diguanylate cyclase, phosphodiesterase, PilZ, second messenger

**Abstract**

*Myxococcus xanthus* has a nutrient-regulated biphasic lifecycle forming predatory swarms in the presence of nutrients and spore-filled fruiting bodies in the absence of nutrients. The second messenger c-di-GMP is essential during both stages of the lifecycle; however, different enzymes involved in c-di-GMP synthesis and degradation as well as several c-di-GMP receptors are important during distinct lifecycle stages. To address this stage specificity, we determined transcript levels using RNA-seq and transcription start sites using Cappable-seq during growth and development at a genome-wide scale. All 70 genes encoding c-di-GMP associated proteins were expressed, with 28 up-regulated and 10 down-regulated during development. In particular, the three genes encoding enzymatically active proteins with a stage-specific function were expressed stage-specifically. By combining operon mapping with published ChIP-seq data for MrpC (Robinson et al., 2014), the CRP-like master regulator of development, we identified nine developmentally regulated genes as regulated by MrpC. In particular, MrpC directly represses expression of *dmxB*, which encodes the diguanylate cyclase DmxB that is essential for development and responsible for the c-di-GMP increase during development. Moreover, MrpC directly activates transcription of *pmxA*, which encodes a bifunctional phosphodiesterase that degrades c-di-GMP and 3', 3' cGAMP *in vitro* and is essential for development. Thereby, MrpC regulates and curbs the cellular pools of c-di-GMP and 3', 3' cGAMP during development. We conclude that temporal regulation of the synthesis of proteins involved in c-di-GMP metabolism contributes to c-di-GMP signaling specificity. MrpC is important for this regulation, thereby being a key regulator of developmental cyclic di-nucleotide metabolism in *M. xanthus.*

**Importance**

The second messenger c-di-GMP is important during both stages of the nutrient-regulated biphasic lifecycle of *Myxococcus xanthus* with the formation of predatory swarms in the presence of nutrients and spore-filled fruiting bodies in the absence of nutrients. However, different enzymes involved in c-di-GMP synthesis and degradation are important during distinct lifecycle stages. Here, we show that the three genes encoding enzymatically active proteins with a stage-specific function are expressed stage-specifically. Moreover, we find that the master transcriptional regulator of development MrpC directly regulates expression of *dmxB*, which encodes the diguanylate cyclase DmxB that is essential for development, and of *pmxA*, which encodes a bifunctional phosphodiesterase that degrades c-di-GMP and 3', 3' cGAMP *in vitro* and is essential for development. We conclude that temporal regulation of the synthesis of

64 proteins involved in c-di-GMP metabolism contributes to c-di-GMP signaling specificity, and that
65 MrpC plays an important role in this regulation.
66
67

## Introduction

In bacteria, signaling by nucleotide-based second messengers have important functions in adaptive responses to environmental changes (1-6). 3'-5', 3'-5 cyclic di-GMP (c-di-GMP) is a versatile second messenger that regulates numerous processes including exopolysaccharide (EPS) synthesis, biofilm formation, cell cycle progression, virulence, motility, and multicellular development (1, 2). c-di-GMP is synthesized by diguanylate cyclases (DGCs), which contain the conserved GGDEF domain, and degraded by phosphodiesterases (PDEs), which contain an EAL or HD-GYP domain (1, 2). The effects of changing c-di-GMP levels are implemented by c-di-GMP binding receptors, which regulate downstream responses at the transcriptional, translational or post-translational level (1, 2). Reflecting the versatility of c-di-GMP, c-di-GMP receptors comprise a variety of proteins with little sequence homology, including enzymatically inactive DGC and EAL domain proteins (7-11), PilZ-domain proteins (12-16), MshEN-domain proteins (17, 18), and proteins of different transcription factor families (19-26). Among these receptors, enzymatically inactive DGC and EAL domain proteins as well as PilZ- and MshEN domains can be bioinformatically predicted (17, 27).

Often individual bacterial genomes encode multiple DGCs, PDEs and c-di-GMP receptors (1). Yet, inactivation of individual genes for DGCs, PDEs and c-di-GMP receptors can result in distinct phenotypes, underscoring that specific signaling modules exist. Thus, a central question is how this signaling specificity is accomplished. Three mutually non-exclusive models have been proposed to explain this specificity (1, 28, 29). Firstly, individual signaling modules can be temporally separated based on differential regulation of their synthesis and/or degradation; secondly, individual signaling modules can be spatially separated by protein complex formation or by localizing to distinct subcellular locations; and, thirdly, effectors of different signaling modules may have different binding affinities for c-di-GMP.

*Myxococcus xanthus* is a model organism for studying social behaviors and cell differentiation in bacteria (30). *M. xanthus* has a nutrient-regulated biphasic life cycle. In the presence of nutrients, cells form predatory swarms that spread coordinately using type IV pilus (T4P)-dependent motility and gliding motility (31, 32). Upon nutrient depletion, *M. xanthus* initiates a developmental program that culminates in the formation of multicellular, spore-filled fruiting bodies while cells that remain outside fruiting bodies differentiate to either so-called peripheral rods or undergo cell lysis (33-35). Nucleotide-based second messengers have important roles during both stages of the lifecycle: During growth, c-di-GMP is important for type IV pili-

dependent motility and for regulation of motility (36, 37). During development, the starvation-induced activation of the stringent response with synthesis of the second messenger (p)ppGpp is required and sufficient to initiate development (38, 39). Moreover, the cellular c-di-GMP level increases dramatically during development, and this increase is essential for completion of development (40). Development also depends on global transcriptional changes (41), regulation of motility (31, 32) and cell-cell signaling (30, 42).

Several transcription factors that are essential for fruiting body formation and sporulation have been identified (41). Among these, MrpC is a member of the cAMP receptor protein (CRP) family of transcription factors (43) and has been referred to as a master regulator of development (41). Currently, no ligand for MrpC has been reported, and MrpC on its own binds target promoters *in vitro* (44-51). MrpC alone is a negative autoregulator (44) and directly activates transcription of *fruA* (45), which encodes a transcriptional regulator that is also essential for development (52, 53). MrpC and FruA jointly regulate the expression of multiple genes during development (46-51).

Systematic inactivation of all 36 genes for GGDEF-domain proteins, EAL-domain proteins, and HD-GYP-domain proteins identified only three enzymatically active proteins that are important during growth and development under standard laboratory conditions. Interestingly, each of the three proteins are important during a distinct stage of the lifecycle. The DGC DmxA is important for T4P-dependent motility in the presence of nutrients but not for development (37, 40). By contrast, the DGC DmxB and the HD-GYP-type PDE PmxA are exclusively important for development (37, 40). DmxB is the DGC responsible for the dramatic increase in the c-di-GMP level during development (40). PmxA degrades c-di-GMP as well as the di-nucleotide 3'-5', 3'-5' cyclic GMP-AMP (cGAMP) *in vitro* and with the highest activity towards cGAMP (40, 54). Lack of PmxA does not lead to significant changes in the c-di-GMP level during development (40) while it remains unknown how lack of PmxA may affect cGAMP accumulation *in vivo*.

Several c-di-GMP receptors have been experimentally verified in *M. xanthus*. The histidine protein kinase SgmT contains an enzymatically inactive GGDEF domain that binds c-di-GMP and works together with the DNA binding response regulator DigR to regulate extracellular matrix composition during growth and development (8, 37). The enhancer binding protein Nla24 also binds c-di-GMP and is important for motility during growth as well as development (40, 55, 56). Systematic inactivation of all 24 genes encoding PilZ-domain proteins identified PixA and

PixB as c-di-GMP receptors that regulate motility (36). While PixA is important only during growth, PixB is crucial during growth and development (36). Finally, the ribbon-helix-helix proteins CdbA and CdbB bind c-di-GMP (57). CdbA is an essential nucleoid-associated protein important for chromosome organization and segregation (57).

With the exception of DmxB, synthesis of which is strongly up-regulated during development (40), it is not understood how c-di-GMP metabolizing enzymes and some verified receptors are functionally restricted to either growth or development. To increase our understanding of c-di-GMP signaling and specificity in *M. xanthus,* we used RNA-seq to determine during which stage(s) of the lifecycle the 70 genes encoding c-di-GMP metabolizing enzymes, potential c-di-GMP receptors and known c-di-GMP receptors (from here on “c-di-GMP associated proteins”) are expressed. We found that all these genes are expressed, and with 28 being up-regulated and 10 down-regulated during development. In particular, transcription of the three genes encoding enzymatically active proteins with a stage-specific function were regulated in a stage-specific manner, supporting that temporal regulation of the synthesis of proteins involved in c-di-GMP metabolism contributes to signaling specificity. To inform the RNA-seq analysis, we performed Cappable-seq to identify transcription start sites (TSSs) at a genome-wide scale. These data together with a previously published ChIP-seq analysis to map MrpC binding sites during development (50) revealed nine of the developmentally regulated genes as candidates for being directly regulated by MrpC. In particular, we found that MrpC directly represses *dmxB* and activates *pmxA* expression. Consistently, a Δ*mrpC* mutant has increased accumulation of c-di-GMP and cGAMP.

## Results

### RNA-seq transcriptome profiling reveals pervasive developmental regulation of genes encoding "c-di-GMP associated proteins"

To elucidate whether transcriptional regulation of genes for "c-di-GMP associated proteins" contributes to their stage-specific function, we performed RNA-seq analyses using the wild-type (WT) strain DK1622. To this end, we collected total RNA from non-starved cells (from here on referred to as 0 h of development) and from cells developed for 6, 12, 18 and 24 h under submerged culture conditions. These time points span the entire process of aggregation of cells to form fruiting bodies and the early stages of sporulation. RNA was isolated from two biological replicates. RNA sample preparation, depletion of rRNA, sequencing and data analysis are described in Materials and Methods. Benchmarking of the RNA-seq data using reverse transcription quantitative PCR (RT-qPCR) analyses of the *mrpC* and *fruA* genes that are both transcriptionally up-regulated during development (43, 44, 52, 53) demonstrated that the two genes had the same expression patterns in the two approaches (Fig. S1).

Subsequently, we focused on the 70 genes encoding "c-di-GMP associated proteins. These genes include all those encoding proteins with a GGDEF domain (18), EAL domain (2), HD-GYP domain (6), PilZ domain (24), or MshEN domain (17) as well as CdbA, CdbB and Nla24. All proteins with one of these domains were included because non-enzymatically proteins or proteins that do not bind c-di-GMP can still be involved in regulation of c-di-GMP-dependent processes (11, 58). All 70 genes were expressed with normalized read counts of more than 50 at all five time points (Fig. 1A, Table S1A). A comparison of transcript levels during development to that during growth (0 h), revealed four clusters with distinct expression profiles. One cluster of ten genes including *dmxB, pmxA* and *pkn1* as well as the benchmarking *mrpC* and *fruA* genes were induced more than 4-fold ($\log_2$FC ≥2, adjusted *p*-value ≤0.05) at one or more time points during development (Fig. 1AB, Table S1B). Pkn1 is a Ser/Thr protein kinase with a C-terminal PilZ domain and is specifically important for development (36, 59); it is not known whether the PilZ domain binds c-di-GMP. These observations are in agreement with previous findings that *dmxB* and *pkn1* transcription is up-regulated during development (40, 59). A second cluster of 18 genes including *tmoK, pixB* and *pilB* were induced more than 2-fold ($\log_2$FC ≥1, adjusted *p*-value ≤0.05) at one or more time point(s) during development. TmoK is a histidine protein kinase with a C-terminal GGDEF domain and is important for T4P-dependent motility during growth as well as for development; the GGDEF domain does not have DGC activity and does not bind c-di-GMP (37, 40). PilB is the ATPase for T4P extension and contains an N-terminal

MshEN domain (17, 60) but it is not known whether it binds c-di-GMP. In the third cluster, ten genes including *dmxA, cdbA* and *cdbB* were down-regulated more than 2-fold ($log_2$FC ≥-1, adjusted *p*-value ≤0.05) at one or more time point(s) during development (Fig. 1B). Expression of the remaining 32 genes, including *sgmT*, *pixA, plpA* and *nla24* were not significantly regulated during development (Fig. 1B, Table S1B). PlpA is a PilZ-domain protein that regulates motility during growth but is not important for development and was reported not to bind c-di-GMP *in vitro* (36, 61). Control experiments using RT-qPCR on the same RNA as for RNA-seq for selected genes (*dmxA*, *dmxB*, *pkn1*) reproduced the RNA-seq data (Fig. S1).

We conclude that expression of the genes for the enzymatically active proteins (DmxA, DmxB and PmxA) with a stage-specific function correlates with that stage of the lifecycle. Similarly, the gene for the developmentally important Pkn1 protein is up-regulated during development while the gene for the growth-related PixA was constitutively expressed. Similarly, the genes for the three verified c-di-GMP receptors (SgmT, PixB, Nla24) that function during both stages of the lifecycle were expressed constitutively while the genes for the essential proteins CdbA and CdbB were down-regulated during development. Altogether, these observations support that transcriptional regulation of genes encoding proteins that act in a stage-specific manner may contribute to temporally restricting their activity.

Genome-wide mapping of transcription start sites using Cappable-seq

To further understand transcriptional regulation of genes for “c-di-GMP associated proteins”, we performed genome-wide mapping of transcription start sites (TSSs) with single-nucleotide-resolution using Cappable-seq (62). For this, total RNA was isolated in two biological replicates from growing *M. xanthus* cells (0 h) and from cells developed for 6, 12, 18 and 24 h under the same conditions as for the RNA-seq analysis. RNA samples were enriched for primary transcripts with a triphosphate at the 5’-end and cDNA libraries generated and sequenced (Materials and Methods). The number of reads starting at a certain position was normalized to the total number of reads to obtain a relative read score (RRS) (Materials and Methods) (Table S2). As in (62), TSS with an RRS <1.5 (equivalent to ~10 reads or less) were discarded from the analysis.

We benchmarked the accuracy of Cappable-seq using the previously mapped TSSs of *fruA* and *mrpC*. For *fruA*, we identified 12 potential TSSs in both biological replicates (Table S3A). The potential TSSs at -235 and -286 relative to the first nucleotide in the start codon (from here on,

TSC for translation start codon) were significantly above the threshold and observed at all time points while the remaining 10 were close to the threshold, and generally not observed at all time points. The signal for the TSS at -235 increased during development while the one at -286 did not (Fig. S2A; Table S3A). A TSS at -235 matched the RNA-seq data (Fig. S2A). Importantly, the TSS at -235 matches the previously identified TSS using primer extension on RNA isolated from developing cells (53). For *mrpC*, two potential TSS were identified (Table S3A). The TSS at -58 bp relative to TSC had the highest score, was detected at all time points in both replicates, and increased during development (Fig. S2B; Table S3A). The potential TSS at -21 relative to the TSC was close to the threshold, and detected only at 12 and 24 h. A TSS at -58 matched the RNA-seq data (Fig. S2B; Table S3A). Importantly, a TSS located at -60 bp relative to TSC was identified using primer extension on RNA from developing cells (63). We conclude that Cappable-seq reproduces previously identified TSS of *fruA* and *mrpC* with good accuracy and also identified alternative potential TSSs. These alternative TTSs are likely explained by the higher sensitivity of Cappable-seq compared to primer extension (62). Further work is needed to verify whether they represent genuine TSSs.

MrpC regulates expression of several genes for “c-di-GMP associated proteins” during development

Having validated the Cappable-seq approach, we aimed to identify the transcriptional units encoding “c-di-GMP associated proteins”. For this, we defined genes likely to be in an operon as those transcribed from the same strand, and with an intergenic distance between stop and start codon of flanking genes ≤50 bp (Table S3C). By combining these data with Cappable-seq data, most genes encoding “c-di-GMP associated proteins” could be divided in four categories: Genes likely not part of an operon (32), likely first gene in an operon (11), likely internal gene in operon (4), and likely internal gene in operon and with an internal promoter (12); for four predicted operons and seven genes predicted not to be in an operon, no TSSs were detected (Table S3BC).

During these analyses, we noticed that several TSSs associated with genes/operons for “c-di-GMP associated proteins” were close to binding site(s) for MrpC as mapped at a genome-wide scale using ChIP-seq on cells developed for 18 h (50). That analysis identified >1500 MrpC binding sites on the *M. xanthus* genome, many of which map to promoter regions of developmentally regulated genes. To identify genes/operons for “c-di-GMP associated proteins” that could potentially be directly regulated by MrpC, we used two criteria. Firstly, we used the

criterion of Robinson *et al.* (50) who identified promoter regions with an MrpC binding site as those in which the MrpC ChIP-seq peak was located at a distance of -400 to +100 bp from a TSC. Secondly, based on published experimental data on MrpC binding to the *fruA* and *mrpC* promoters (44, 45, 64), we included the criterion that an MrpC ChIP-seq peak should be located within a distance of 200 bp from a TSS (Fig. S2AB). Based on these criteria, we identified 18 operons/genes for "c-di-GMP associated proteins" that could potentially be regulated by MrpC (Table 3BC). Using RT-qPCR, we found that two (*dmxB* and MXAN_7500) and seven (MXAN_1525, *pmxA*, MXAN_4232, *pkn1*, MXAN_2902, MXAN_6957, MXAN_7024) of these 18 genes were expressed at higher and lower levels, respectively in the Δ*mrpC* mutant compared to WT while nine genes displayed similar expression patterns in the two strains (Fig. 2; Fig. S3). The observation that nine of the candidate genes were not expressed in an MrpC-dependent manner under the conditions tested are in agreement with the possibility that the relevant MrpC ChIP-seq peaks may represent false positives as discussed by Robinson *et al.* We note that the expression of all tested genes in the WT as measured by RT-qPCR matches the expression patterns obtained using RNA-seq (Fig. 1B). The nine differentially expressed genes include six of the most highly developmentally up-regulated genes for "c-di-GMP associated proteins" (Fig. 1B). These results support that MrpC is a negative regulator of *dmxB* and MXAN_7500 expression and a positive regulator of MXAN_1525, *pmxA*, MXAN_4232, *pkn1,* MXAN_2902, MXAN_6957 and MXAN_7024 expression. From here on, we focused on MrpC regulation of *dmxB* and *pmxA*, which encode enzymatically active proteins that are specifically important for development.

MrpC negatively regulates *dmxB* expression and DmxB accumulation

Based on our criteria as well as RNA-seq, *dmxB* forms a two-gene operon with the downstream gene MXAN_3734 (Fig. 3A; Fig. S4; Table S3BC). We identified seven potential TSSs upstream of *dmxB* in both replicates (Table S3BC). Among these, we focused on four with high scores in both replicates at several time points (Fig. 3B), while the remaining three had low scores and each appeared at only one time point (Table S3BC). The TSS at -297 relative to TSC was detected with the highest score at all time points and increased as development progressed (Fig. 3B, Table S3BC). The TSS at -213 was the second highest scoring and sharply increased at 18 h. The TSSs at -171 and -135 did not significantly change in score over time. A comparison of Cappable-seq and RNA-seq data supports that TSSs at -297 and -213 are genuine TSSs (Fig. 3B; Fig. S4). These data support that *dmxB* is transcribed from multiple promoters, and those with TSSs at -297 and -213 are developmentally regulated.

The *dmxB* promoter region contains an MrpC ChIP-seq peak centered at -388 bp relative to TSC (Fig. 3BC; Table S3BC). To test whether MrpC directly binds to the upstream region of *dmxB*, we performed an electrophoretic mobility shift assay (EMSA) using a PCR-amplified 480 bp Hexachloro-fluorescein (Hex)-labeled PCR product that extends from 92 bp upstream of the ChIP-seq peak coordinate to the *dmxB* TSC (Fig. 3C). Titrating purified $His_6$-MrpC (Fig. S5) against the Hex-labelled probe resulted in the formation of one well-defined shifted band consistent with one binding site for MrpC in the *dmxB* promoter region (Fig. 3D).

We identified four potential MrpC binding sites (BS1-4) in the *dmxB* promoter region using the consensus sequence defined by (50) (Fig. 3C). We prepared four Hex-labelled *dmxB* promoter fragments each containing substitutions of conserved bp in one of the four potential MrpC binding sites as described (44). In EMSA experiments, the fragments with substitutions in BS1, BS2 or BS3 bound MrpC as the WT fragment (Fig. 3E). By contrast, the fragment with a mutated BS4 did not bind MrpC (Fig. 3E). Based on these data, we suggest that *dmxB* promoter contains one binding site, i.e. BS4, for MrpC centered at -409 and, thus, close to the MrpC ChIP-seq peak centered at -388 bp (Fig. 3C).

To test the impact of MrpC and its binding to BS4 on *dmxB* promoter activity *in vivo*, we constructed fluorescent reporters in which the WT *dmxB* promoter fragment ($P_{dmxB}^{WT}$) used in the EMSA experiments or the same fragment with a mutated BS4 ($P_{dmxB}^{BS4*}$) were fused to the start codon of *mCherry* and ectopically expressed from the Mx8 *attB* site. As a negative control, *mCherry* without the *dmxB* promoter was fused to *mCherry*. In agreement with the RT-qPCR data (Fig. 2), mCherry expressed from $P_{dmxB}^{WT}$ accumulated at significantly higher levels in the Δ*mrpC* mutant compared to WT at all tested time points (Fig. 3F). Importantly, the activity of $P_{dmxB}^{BS4*}$ was significantly higher than that of $P_{dmxB}^{WT}$ in WT (Fig. 3G). We conclude that MrpC binds to BS4 to repress *dmxB* expression.

Finally, we observed that DmxB was detected at low levels at 0 h in WT and its accumulation increased during development (Fig. 3H) as previously observed (40). Importantly, DmxB accumulated at significantly higher levels at all time points in the Δ*mrpC* mutant compared to WT (Fig. 3H) consistent with MrpC acting as a repressor of *dmxB* transcription.

<u>MrpC positively regulates *pmxA* expression and PmxA accumulation</u>

Based on our criteria, *pmxA* is the last gene of a three gene operon (Fig. 4A). Based on Cappable-seq, there is one TSS at -63 relative to the TSC of MXAN_2063, and three TSSs immediately upstream of *pmxA* (Fig. 4B; Table S3BC). RT-PCR analysis on RNA isolated from WT at 0 and 6 h of development support that MXAN_2063-MXAN_2062-*pmxA* is transcribed as an operon at both time points (Fig. S6A). The three genes were barely expressed at 0 h; at later time points, MXAN_2063 and MXAN_2062 expression remained low while *pmxA* expression increased (Fig. 4B; Fig. S6B). Accordingly, the score for the single TSS upstream of MXAN_2063 remained low (Fig. 4B; Table S3C). The TSSs upstream of *pmxA* had scores close to the threshold (Table S3BC). Therefore, we analyzed each biological replicate separately (Fig. 4B, right panels; Table S3BC). A TSS at -226 relative to the TSC of *pmxA* was detected at all time points and was not developmentally regulated while a TSS at -131 was detected at 6 h and later suggesting developmental up-regulation. A TSS at -53 was detected only at 24 h. We conclude that the MXAN_2063-MXAN-2062-*pmxA* operon is transcribed from a promoter upstream of MXAN_2063 during growth and development; in addition, *pmxA* is transcribed from internal promoters, two of which are developmentally regulated.

We identified a single MrpC ChIP-seq peak centered at -210 upstream of the *pmxA* TSC and none upstream of MXAN_2063 suggesting that MrpC is involved in activation of the internal promoter(s) during development (Fig. 4BC). In EMSA experiments with a 310 bp Hex-labeled probe (Fig. 4C), 0.1 μM $His_6$-MrpC gave rise to a single well-defined shifted band, and at 0.5-2.0 μM $His_6$-MrpC, an additional well-defined shifted band was evident (Fig. 4D). We identified three potential MrpC binding sites (BS1-3) upstream of *pmxA* (Fig. 4C), mutated them separately, and tested $His_6$-MrpC binding to the mutated promoters. The $P_{pmxA}^{WT}$ fragment gave rise to two shifted bands at 1.0 μM $His_6$-MrpC, while the fragments containing substitutions in BS1 or BS2 generated only one shifted band, the fragment with substitutions in BS3 behaved as $P_{pmxA}^{WT}$, and a fragment with both BS1 and BS2 mutated did not bind MrpC at 1.0 μM (Fig. 4C, 4E). We conclude that MrpC binds to the internal *pmxA* promoter region at two sites, BS1 and BS2, centered at -191 and -232 relative to the TSC of *pmxA* (Fig. 4C).

The importance of MrpC and its binding to BS1 and BS2 on *pmxA* promoter activity *in vivo* was tested as described for $P_{dmxB}$ using the same fragments as in the EMSA experiments. mCherry expressed from $P_{pmxA}^{WT}$ was detected in immuno-blots of WT at 0, 3 and 6 h, and at significantly reduced levels in the Δ*mrpC* mutant at 3 and 6 h (Fig. 4F) in agreement with the RT-qPCR

362 experiments (Fig. 2). Importantly, the activity of $P_{pmxA}^{BS1*}$, $P_{pmxA}^{BS2*}$ and $P_{pmxA}^{BS1*/BS2*}$ was
363 significantly lower than that of $P_{pmxA}^{WT}$ in WT (Fig. 4G).
364
365 To determine PmxA levels during development, we used an active PmxA-mVenus fusion (Fig.
366 S6C) expressed from the native site. Surprisingly, the level of PmxA-mVenus did not increase
367 significantly during development in WT (Fig. 4H) despite transcription being up-regulated ~4-fold
368 during development (Fig. 1B, 2B and Fig. 4F). Importantly, the level of PmxA-mVenus in the
369 Δ*mrpC* mutant was significantly reduced compared to WT at all time points (Fig. 4H). Altogether
370 these observations support that *pmxA* is transcribed from a promoter upstream of MXAN_2063
371 as well as from internal promoter(s), which are activated by MrpC by binding to BS1 and BS2.
372
373 MrpC curbs accumulation of c-di-GMP and 3', 3' cGAMP during development
374 Next, we investigated the functional consequences of altered accumulation of DmxB and PmxA
375 with respect to cyclic di-nucleotides in the Δ*mrpC* mutant. As described (40), the c-di-GMP level
376 increased significantly during development in a DmxB-dependent manner in the WT (Fig. 5A). In
377 agreement with the accumulation profile of DmxB, the c-di-GMP level was slightly but
378 significantly higher in the Δ*mrpC* mutant than in the WT at 0 h, and significantly higher during
379 development in the Δ*mrpC* mutant, and the extra c-di-GMP was dependent on DmxB (Fig. 5A).
380
381 Because recent studies revealed that PmxA activity against c-di-GMP is significantly lower than
382 towards cGAMP (54), we measured c-di-GMP as well as cGAMP levels in WT and the Δ*pmxA*
383 and Δ*mrpC* mutants. As previously shown (40), the c-di-GMP level in the WT and the Δ*pmxA*
384 mutant were similar (Fig. S7). The cGAMP level increased significantly during development in
385 WT (Fig. 5B). Importantly, in the Δ*pmxA* mutant, the cGAMP level was significantly higher than
386 in WT during growth (0 h) as well as development, consistent with the accumulation profile of
387 PmxA-mVenus and PmxA having PDE activity against cGAMP *in vivo* (Fig. 4H). The cGAMP
388 level in the Δ*mrpC* mutant was significantly higher than in WT at all time points and, except at 0
389 h, largely similar to that in the Δ*pmxA* mutant. Finally, the Δ*pmxA*Δ*mrpC* mutant accumulated
390 cGAMP similarly to the Δ*pmxA* mutant documenting that the increased cGAMP level in the
391 Δ*mrpC* mutant depends on PmxA.
392
393 We conclude that MrpC by regulating the expression of *dmxB* and *pmxA* controls the cellular
394 pools of c-di-GMP and cGAMP.
395

396 Aggregated and non-aggregated cells accumulate MrpC, DmxB, PmxA-mVenus as well as c-di-
397 GMP or cGAMP at similar levels
398 In the DZ2 WT strain, MrpC expression and accumulation are higher in aggregated cells, i.e.
399 cells that differentiate to spores within fruiting bodies, compared to non-aggregated cells, i.e.
400 cells that differentiate to peripheral rods (33, 44) raising the possibility that c-di-GMP and/or
401 cGAMP might also accumulate at different levels in these cell types. To this end, we developed
402 DK1622 WT cells under submerged conditions and then separated aggregated and non-
403 aggregated cells at 24 and 48 h of development and determined MrpC, DmxB, PmxA-mVenus,
404 c-di-GMP and cGAMP levels in the two cell types. As a control for proper cell separation, we
405 used accumulation of Protein C, which accumulates in aggregated cells and at a much-reduced
406 level in non-aggregated cells (65). In WT as well as in WT producing PmxA-mVenus, cells were
407 properly separated based on the level of Protein C (Fig. 6A). Surprisingly, at both time points,
408 MrpC accumulated at similar levels in the two cell types (Fig. 6A). Consistently DmxB and
409 PmxA-mVenus accumulated at similar levels in the two cell types (Fig. 6A) and c-di-GMP (Fig.
410 6B) as well as cGAMP (Fig. 6C) levels were similar in the two cell types at both time points.
411 These observations support that MrpC, DmxB, PmxA, c-di-GMP and cGAMP are not involved in
412 cell fate determination during development in DK1622 WT.
413

## Discussion

Here, we present a comprehensive analysis of the expression of genes encoding "c-di-GMP associated proteins" in *M. xanthus*. This analysis was motivated by previous observations that lack of several of these proteins cause defects during only one of the stages of the biphasic life cycle while others cause defects during both stages. Using RNA-seq, we found that all these genes were expressed during the lifecycle. More importantly, expression of 28 genes encoding "c-di-GMP associated proteins" was up-regulated, 10 down-regulated, and 32 did not change expression during development. By combining Cappable-seq with data from previously published ChIP-Seq analyses of the CRP-like transcription factor MrpC (50), we identified nine genes for "c-di-GMP associated proteins" that are regulated (directly or indirectly) by MrpC. Among these, detailed analyses revealed that (1) MrpC binds to and represses the promoter(s) of *dmxB*, which encodes the DGC DmxB that is essential for development and responsible for the dramatic increase in c-di-GMP during development; and (2) MrpC binds to and activates internal promoter(s) in the MXAN_2063-MXAN_2062_*pmxA* operon to promote transcription of *pmxA*, which encodes a PDE that is essential for development. Thereby, MrpC regulates the cellular pools of c-di-GMP and cGAMP. Altogether, our findings support that differential expression of genes for "c-di-GMP associated proteins" contribute to their stage-specific function. Moreover, we conclude that MrpC is important for the temporal regulation of genes for c-di-GMP synthesis and cGAMP degradation, and a key regulator of cyclic nucleotide metabolism in *M. xanthus*.

Expression of *dmxB* and DmxB accumulation are up-regulated during development (37, 40). Consistently, lack of DmxB DGC activity only causes developmental defects. We found that *dmxB* is likely expressed from four promoters, two of which are developmentally up-regulated and two constitutively expressed at low levels (Fig. 7). MrpC is not important for up-regulation of *dmxB* transcription during development; rather MrpC represses transcription of *dmxB* during growth and development. Based on EMSA analyses, MrpC binds to a single site (BS4) centered at -409 relative to the TSC to accomplish this function. The MrpC binding site is located 112, 196, 238 and 274 bp upstream from the four TSSs (Fig. 7); however, from our current analyses, we do not know which promoter(s) is repressed by MrpC. The distance between the MrpC binding sites and the four TSSs strongly argues that MrpC does not directly block binding of the RNA polymerase. Recently, McLaughlin *et al.* (44) elegantly demonstrated that MrpC functions as a negative autoregulator of the *mrpC* promoter by outcompeting binding of the MrpB transcriptional activator, which is an enhancer binding protein. We speculate that MrpC may

function by a similar mechanism in *dmxB* expression. However, the activator of *dmxB* developmental expression remains to be identified. The MrpC-dependent repression of *dmxB* expression curbs DmxB synthesis and, consequently, c-di-GMP accumulation slightly during growth and more significantly during development. We previously showed that an increase in the global pool of c-di-GMP is essential for development; however, further increasing this level does not interfere with development (40) arguing that the increased c-di-GMP pool in the Δ*mrpC* mutant may not significantly contribute to the developmental defects in this mutant. Rather we suggest that the importance of the negative regulation of *dmxB* expression by MrpC lies in avoiding futile synthesis of DmxB and c-di-GMP.

Lack of PmxA only causes developmental defects. Consistently, expression of *pmxA* is up-regulated during development. *pmxA* is part of a three gene operon, which is expressed a low levels during growth and development. In addition, *pmxA* is expressed from three internal promoters, two of which are developmentally up-regulated (Fig. 7). Our data suggest that the developmental up-regulation of *pmxA* expression derives from the internal promoters. MrpC is essential for up-regulation of *pmxA* transcription; and, based on EMSA analyses, MrpC binds to two sites (BS1 and BS2) centered at -191 and -232 relative to the TSC. Because BS1 only has one mis-match compared to the consensus MrpC binding site while BS2 has two (Fig. 4C), we suggest that MrpC binds BS1 with a higher affinity than BS2. From our current analyses, we do not know which of the internal promoters are activated by MrpC. However, based on a comparison to CRP-activated promoters in *Escherichia coli* (66) and the distance between the MrpC binding sites and the TSSs, we speculate that the promoter with a TSS at -131 relative to the TSC could be activated by MrpC. In the case of the promoter with a TSS at -53, the distance to the MrpC binding sites makes it less likely that this promoter is directly activated by MrpC; however, we notice that CRP in *Escherichia coli* can act as a as a structural element from long distances together with an additional transcriptional activator as in the case of the *malK* promoter (67). It is also a possibility that the promoter with a TSS at -53 is activated by MrpC together with FruA as described for several developmentally regulated promoters (46-51). While transcription of *pmxA* is up-regulated during development in WT, the level of PmxA accumulation (as measured using an active PmxA-mVenus fusion) does not change significantly. By contrast, in the Δ*mrpC* mutant, *pmxA* transcription is not up-regulated and PmxA accumulation is strongly decreased. These observations indicate that PmxA accumulation is not only regulated at the transcriptional level but also at the translational and/or post-translational level. PmxA is essential for development arguing that the reduced *pmxA*

482 expression and PmxA accumulation in the Δ*mrpC* mutant contributes to the developmental
483 defects in this mutant. However, the developmental defects of the Δ*mrpC* mutant are more
484 severe than in the case of the Δ*pmxA* mutant (43, 68) supporting that reduced PmxA
485 accumulation alone does not explain the developmental defects in the Δ*mrpC* mutant.
486
487 PmxA is a PDE with higher activity towards cGAMP than c-di-GMP (40, 54). Accordingly, the
488 cellular pool of c-di-GMP is unaltered in a Δ*pmxA* mutant compared to WT. We found that the
489 level of cGAMP increased during development of WT; importantly, the cGAMP level was
490 significantly higher in the Δ*pmxA* mutant compared to WT. Similarly, we found that the cGAMP
491 pool is highly increased in the Δ*mrpC* mutant. These data for the first time show that cGAMP
492 accumulates in *M. xanthus in vivo* and also provide evidence that PmxA is directly involved in its
493 degradation *in vivo*. We speculate that a low concentration of cGAMP maintained by PmxA
494 might be important for development. In *M. xanthus*, GacA and GacB both belong to the Hypr
495 subfamily of GGDEF domain proteins that synthesize cGAMP rather than c-di-GMP *in vitro* (69).
496 Lack of GacA or GacB does not cause evident phenotypes during growth and development (37,
497 40) but the cGAMP level in these mutants is not known. Based on the RNA-seq data, *gacA* is
498 up-regulated two-fold during development while *gacB* is constitutively expressed (Fig. 1B) and
499 none of these two genes appear to be regulated by MrpC. In future experiments, it will
500 interesting to analyze development and the cGAMP level in a Δ*gacA* Δ*gacB* double mutant to
501 determine whether cGAMP is important for development.
502
503 In addition to *dmxB* and *pmxA*, MrpC positively or negatively regulates expression of seven
504 genes for “c-di-GMP signaling proteins” during development (Fig. 1B, Fig. 2). Among these, only
505 the gene for Pkn1, which is up-regulated in an MrpC-dependent manner during development,
506 has been shown to be important for development and none for growth (36, 59) suggesting that
507 lack of Pkn1 may also contribute to the developmental defects in the Δ*mrpC* mutant.
508 Interestingly, we found that some of the MrpC-regulated genes are also differentially expressed
509 during growth. Along these lines, DmxB and PmxA accumulation was increased and decreased,
510 respectively and the levels of c-di-GMP and cGAMP increased during growth in the Δ*mrpC*
511 mutant. The significance of these observations is not clear because lack of MrpC was reported
512 to only cause developmental defects (43). Nevertheless, they indicate that MrpC accumulates
513 during growth but has its primary function in development.
514

The DGC DmxA is only important during growth (37, 40) and its gene is transcriptionally down-regulated during development. Based on the mapped MrpC ChIP-seq peaks, this down-regulation is independent of MrpC. The reciprocal regulation of *dmxA* and *dmxB* together with the up-regulation of *pmxA*, support a model whereby the signaling specificity of enzymatically active DGCs and PDE with discrete functions during growth and development relies on their temporally regulated synthesis. By contrast, no clear picture emerges for the experimentally verified c-di-GMP receptors regarding transcription of the involved genes: The genes for Nla24, SgmT and PixB that all function during growth and development, are constitutively expressed (*nla24* and *sgmT*) or up-regulated (*pixB*); the gene for PixA, which functions during growth, is constitutively expressed. Clearly, more work is needed to understand how these receptors are regulated and their function restricted to certain stages of the lifecycle.

During development, *M. xanthus* adopts three different cell fates, i.e. peripheral rods, spores or cell lysis. Previous experiments using the WT strain DZ2 demonstrated that MrpC accumulates in aggregated cells that differentiate to spores but at a much-reduced level in non-aggregated cells that differentiate to peripheral rods (33). Because c-di-GMP drives cell fate determination in *Caulobacter crescentus* (70), we speculated that c-di-GMP and/or cGAMP could also play a role in cell fate determination in *M. xanthus*. We found that developing cells of the WT strain DK1622 also segregate into aggregated and non-aggregated cells based on the cell type-specific accumulation of Protein C; however, in this WT strain, MrpC as well as DmxB, PmxA-mVenus, c-di-GMP and cGAMP accumulated at similar levels in the two cell types. These observations argue that MrpC, DmxB, PmxA, c-di-GMP and cGAMP are not involved in cell fate determination during development in DK1622.

**Acknowledgements**

We thank Dr. Dobromir Szadkowski for helping with MATLAB scripts, and Dr. Dorota Skotnicka as well as Dr. Anke Treuner-Lange for many helpful discussions. We deeply acknowledge the assistance of the Research Service Centre Metabolomics at the Hannover Medical School in the determination of c-di-GMP and cGAMP levels and the Max Planck Genome Centre Cologne (https://mpgc.mpipz.mpg.de/home) for RNA-seq library construction and sequencing. We acknowledge technical assistance by the Bioinformatics Core Facility at the professorship of Systems Biology at JLU Giessen and the provision of computer resources and general support by the BiGi service center (BMBF grant 031A533) within the de.NBI network. This work was also generously supported by the Deutsche Forschungsgemeinschaft (DFG; German Research Council) within the framework the SPP1879 “Nucleotide second messenger signaling in bacteria” as well as by the Max Planck Society.

**Conflict of Interest**

The authors declare no conflict of interest.

**Data Availability**

All data supporting this study are available within the article, the Supplementary Information files, or at EBI Arrayexpress (http://www.ebi.ac.uk/arrayexpress; RNA-Seq E-MTAB-11043, Cappable-Seq E-MTAB-11042).

**Code availability**

Code for the Cappable-Seq analysis and the Curare version used for the RNA-Seq analysis can be found at Zenodo (www.zenodo.org, ID: 5541852).

**Author contributions**

S.K., D.M., A.B. and L.S.-A. conceptualized the study.
S.K., P.B., D.M. and A.G. performed bioinformatics studies.
S.K. performed genetic and molecular microbiology experiments.
S.K. and L.S.-A. wrote the original draft of the manuscript.
All authors reviewed and edited the original manuscript and approved the final version of the manuscript.
AB, AG and L.S.-A. acquired funding and provided supervision.

## Materials and Methods

Cultivation of *M. xanthus* and *E. coli*. All *M. xanthus* strains used in this study are derivatives of WT DK1622 (71). In-frame deletions were generated as described (72). All plasmids were verified by sequencing. All strains were confirmed by PCR. *M. xanthus* strains, plasmids and oligonucleotides used are listed in Table 1, Table 2, and Table S4, respectively. *M. xanthus* cells were grown at 32°C in 1% CTT broth (1% Bacto Casitone (Gibco), 10 mM Tris-HCl pH 8.0, 1 mM $KPO_4$ pH 7.6, 8 mM $MgSO_4$) (73) or on 1% CTT 1.5% agar plates with addition of kanamycin (40 μg $ml^{-1}$) or oxytetracycline (10 μg $ml^{-1}$) if relevant. *E. coli* cells were cultivated in LB (74) or on LB 1.5% agar plates at 37ºC with addition of kanamycin (40 μg $ml^{-1}$) or tetracycline (10 μg $ml^{-1}$) if relevant. All plasmids were propagated in *E. coli* Top10 (Invitrogen™ life technologies) unless otherwise mentioned.

Development under submerged conditions and cell separation. Exponentially growing *M. xanthus* in CTT were harvested at 5,000 *g* for 5 min and resuspended in MC7 buffer (10 mM MOPS pH 6.8, 1 mM $CaCl_2$) to $7\times10^9$ cells $ml^{-1}$. 1 ml of concentrated cells was added to 10 ml of MC7 buffer in a polystyrene Petri dish with a diameter of 9.2 cm (Sarstedt). For separation of aggregated and non-aggregated cells during development, cells were developed as described and separated following the procedure of (33). Cells were visualized using a Leica DMi8 inverted microscope with Leica DFC280 camera. To determine sporulation efficiency, cells at 120 h of development were harvested, sonicated for 1 min (30% pulse; 50% amplitude with a UP200St sonifier and microtip; Hielscher) to disperse fruiting bodies and then incubated at 55°C for 2 h. Sporulation efficiency was calculated as the number of sonication- and heat-resistant spores formed after 120 h of development, relative to the WT. Spores were counted in a counting chamber (depth, 0.02mm; Hawksley).

RNA sequencing. Total RNA from *M. xanthus* cells developed under submerged conditions was extracted from cells using TRI Reagent (Sigma-Aldrich) according to the manufacturer's protocol. Purified RNA was treated with TURBO DNA-free™ Kit (Invitrogen) according to the manufacturer's protocol. RNA integrity was analyzed by 1% agarose gel electrophoresis. For all samples rRNA depletion, library preparation and sequencing were performed at the Max-Planck-Genome-Centre Cologne, Germany (https://mpgc.mpipz.mpg.de/home/). rRNA depletion was conducted with 1 μg total RNA using Ribo-Zero rRNA Removal Kit Bacteria (Illumina), followed by library preparation with NEBNext Ultra Directional RNA Library Prep Kit for Illumina (New England Biolabs). Library preparation included 11 cycles of PCR amplification. Quality and

quantity were assessed at all steps via capillary electrophoresis (TapeStation, Agilent Technologies) and fluorometry (Qubit, Thermo Fisher Scientific). Sequencing was performed on HiSeq 3000 (Illumina) with 1× 150 bp single reads. Libraries were re-sequenced until a sufficient number of reads were obtained. Sequencing files can be downloaded from EBI ArrayExpress under accession number E-MTAB-11043.

Cappable-sequencing. Total RNA was isolated from *M. xanthus* cells developed under submerged conditions as described. Library preparation and sequencing was performed at Vertis Biotechnologie AG, Freising, Germany (https://www.vertis-biotech.com/home) as described in (62). Briefly, 5' triphosphorylated RNA was capped with 3'-desthiobiotin-TEG-guanosine 5' triphosphate (DTBGTP) (New England Biolabs) using the vaccinia capping enzyme (VCE) (New England Biolabs). Then biotinylated RNA molecules were captured using streptavidin beads and eluted with a biotin-containing buffer. RNA samples were poly(A)-tailed using poly(A) polymerase. Then the 5'-PPP or CAP structures were converted to 5'-P using CAP-Clip Acid Pyrophosphatase (Cellscript). Afterwards, an RNA adapter was ligated to the newly formed 5'-monophosphate structures. First-strand cDNA synthesis was performed using an oligo(dT)-adapter primer and M-MLV reverse transcriptase. The resulting cDNAs were PCR-amplified using a proof-reading enzyme. The libraries were amplified in 15 cycles of PCR. The generated cDNA libraries were sequenced on an Illumina NextSeq 500 system using 75 bp read length. Sequencing files can be downloaded at EBI ArrayExpress under accession number E-MTAB-11042.

Organism. The genome and annotation of *Myxococcus xanthus* DK 1622 (NC_008095.1, downloaded 28.01.2019) were used for all analyses.

RNA-seq analysis. All sequencing runs of one sample were concatenated using "cat" (GNU coreutils 8.30). As reverse transcription is part of the sequencing protocol, this was compensated for by "reverse_complement" of the FASTX-Toolkit 0.0.14 (http://hannonlab.cshl.edu/fastx_toolkit). The differential gene expression analysis was done using the RNA-seq pipeline Curare 0.2.1. This software will be described in details in a separate manuscript. Briefly, the reads were aligned using Bowtie2 2.4.2 in 'very-sensitive' mode and with '--mm' option (75). Except for the WT_t24_2 sample, all samples had mapping rates higher than 90% (Table S5). The resulting SAM/BAM files were processed with Samtools 1.12 (76). The subsequent assignment of mapped reads to genome features was done using the

featureCounts (77) of the subread 2.0.1 package (78). featureCounts was run with "-s 1" settings assigning reads strand specific to the 'gene' features. For every sample, more than 93% of all reads could be assigned to a 'gene' feature (Table S6). Finally, the differential gene expression was analyzed with DESeq2 1.30.1 (79). The Curare version of this analysis can be downloaded at Zenodo (DOI: 10.5281/zenodo.5541852). The count table and mapping results can be downloaded from EBI ArrayExpress under accession number E-MTAB-11043.

Cappable-seq analysis. The TSS pipeline in (62) was used for TSS detection with modifications. This modified pipeline will be described in detail in a separate manuscript. Briefly, the raw Cappable-seq reads were mapped with Bowtie2 2.4.1 using '--all', '--mm', and '--very-sensitive' settings (75). As in the RNAseq analysis, all samples except WT_t24_2 had a mapping rate of >90% (Table S7). A custom script was used to filter all non-best mappings of each read (two equal good mappings will be counted as half a read/mapping each). Created SAM and BAM files were processed using Samtools 1.12 (76) and Pysam 0.16 (https://pysam.readthedocs.io/). Only the first base of each mapping was used for building' alignments per base' scores (Rns) and every following step. The following formula, altered from (62), was used to normalize these scores: RRS = (Rns/Rt) * 1,000,000 (RRS: relative read score, Rt: total number of reads mapped). As in (62), an RRS of 1.5 was used as the lower threshold. The first mapped nucleotide from the sequencing reads identifies the orientation and position of the first nucleotide of the primary transcript. TSSs within three nucleotides were clustered into one TSS. In case of flanking clusters or TSSs within a distance of three or less nucleotides, these were merged into one large cluster. The TSS with the highest RRS in a cluster was defined as the major TSS and used in these analyses. The complete pipeline can be downloaded at Zenodo (DOI: 10.5281/zenodo.5541852). The mapping and TSS results can be downloaded from EBI ArrayExpress under accession number E-MTAB-11042.

RT-qPCR. 1 µg of total RNA isolated as described above was used to synthesize cDNA with the High Capacity cDNA Reverse Transcription Kit (Applied Biosystems) according to the manufacturer's protocol. cDNA templates were diluted 10-fold, 2 µl of a diluted sample was used as a template for RT-qPCR reaction, which contained 1× SYBR Green PCR Master Mix (Applied Biosystems), 2.5 µM of each primer and $H_2O$ to a final volume of 25 µl. A 7500 Real time PCR detection system (Applied Biosystems) was used for RT-qPCR measurements using standard conditions. Experiments were done in two biological replicates, each in two technical replicates. Relative gene expression levels were calculated using the comparative Ct method.

675

676 Operon mapping. RNA preparation was done as described. Primers used are listed in Table S4,
677 and used on genomic DNA, RNA without addition of reverse transcriptase, and cDNA.
678
679 Immuno-blot analysis. Immunoblots were carried out as described (74). Rabbit polyclonal α-
680 DmxB (1:1000 dilution) (40), α-GFP (Roche, 1:2000 dilution), α-mCherry (Biovision, 1:2000
681 dilution), α-protein C (1:2000 dilution) (80) and α-PilC (1:5000 dilution) (81) antibodies were
682 used together with horseradish-conjugated goat anti-rabbit immunoglobulin G (Sigma-Aldrich) or
683 anti-mouse sheep IgG antibody (GE Healthcare) as secondary antibody. Blots were developed
684 using Luminata crescendo Western HRP Substrate (Millipore) and visualized using a LAS-4000
685 luminescent image analyzer (Fujifilm). To quantify immuno-blots, signal intensities of the
686 relevant protein bands were quantified using Fiji (82) and normalized relative to the PilC loading
687 control from the same blot. All immuno-blots were performed in three independent biological
688 replicates.

689 Protein purification. To purify $His_6$-MrpC, *E. coli* Rosseta 2 (DE3)/pLysS strain (Novagen) was
690 transformed with pPH158 (33). The culture was grown in 1L LB with addition of chloramphenicol
691 and kanamycin at 37ºC to an optical density at 600 nm of 0.5-0.7. Protein expression was
692 induced by addition of isopropylthio-β-galactoside (IPTG) to a final concentration of 0.5 mM for 3
693 h at 37ºC. Cells were harvested by centrifugation at 5,000*g* for 10 min at 4ºC and resuspended
694 in lysis buffer (50 mM $NaH_2PO_4$, 300 mM NaCl, 5 mM $MgCl_2$, 10 mM imidazole, 5% glycerol, pH
695 8.0 and Complete Protease Inhibitor Cocktail Tablet (Roche)). Cells were disrupted using a
696 French press and harvested at 48,000*g* for 40 min at 4ºC. The cleared supernatant was filter
697 with 0.45 µm sterile filter (Millipore Merck, Schwalbach) and applied to column with 2 ml of $Ni^{2+}$-
698 NTA-agarose (GE Healthcare) equilibrated with wash buffer (50 mM $NaH_2PO_4$, 300 mM NaCl, 5
699 mM $MgCl_2$, 50 mM imidazole, 5% glycerol, pH 8.0). Protein was eluted with elution buffer (50
700 mM $NaH_2PO_4$, 300 mM NaCl, 5 mM $MgCl_2$, 100-500 mM imidazole, 5% glycerol, pH 8.0).
701 Fractions containing purified $His_6$-MrpC were combined and loaded onto a HiLoad 16/600
702 Superdex 200 pg (GE Healthcare) size exclusion chromatography column equilibrated with lysis
703 buffer without imidazole. Fractions containing $His_6$-tagged MrpC were frozen in liquid nitrogen
704 and stored at −80°C.

705

706 Electrophoretic mobility shift assay (EMSA). Hex-labelled probes were generated using the
707 primer pairs listed in Table S4 and plasmids containing the WT or mutant promoters as

templates. Assays were performed as described (83). Briefly, purified $His_6$-MrpC was mixed at the indicated concentrations with 6 nM (*dmxB* fragments) or 10 nM (*pmxA* fragments) of HEX-labeled DNA fragment in reaction buffer (10 mM Tris pH 8.0, 50 mM KCl, 1 mM DTT, 10 µg $ml^{-1}$ BSA, 10% glycerol, 0.5 µg herring sperm DNA (Thermo Fisher Scientific)) in a total volume of 10 µl, and incubated for 15 min at 20°C. Reaction samples were separated on a 5% polyacrylamide gel in 0.5× TBE (45 mM Tris, 45 mM Borate, 1 mM EDTA) for 1.5 h. Gels were imaged using a Typhoon Phosphoimager (GE Healthcare).

c-di-GMP and cGAMP quantification. To quantify the c-di-GMP and cGAMP levels, cells were grown in CTT or developed under submerged conditions as described. Cells were harvested at 2,500*g* for 20 min at 4°C, lysed in extraction buffer (HPLC grade acetonitrile/methanol/water (2/2/1, v/v/v)), and supernatants evaporated to dryness in a vacuum centrifuge. Pellets were dissolved in HPLC grade water and analyzed by LC-MS/MS. c-di-GMP and cGAMP quantification was performed at the Research Service Centre Metabolomics at the Hannover Medical School, Germany. Experiments were done in three biological replicates. Protein concentrations were determined in parallel using a Pierce®Microplate BCA Protein Assay Kit (Thermo Scientific).

Bioinformatics. Heatmaps were created using R package pheatmap (https://cran.r-project.org/web/packages/pheatmap/index.html). Protein domains were identified using Pfam v33.1 (pfam.xfam.org) (84); signal peptides were predicted with SignalP 5.0 (www.cbs.dtu.dk/services/SignalP-5.0) (85).

## References


1. Römling U, Galperin MY, Gomelsky M. 2013. Cyclic di-GMP: the first 25 years of a universal bacterial second messenger. Microbiol Mol Biol Rev 77:1-52.
2. Jenal U, Reinders A, Lori C. 2017. Cyclic di-GMP: second messenger extraordinaire. Nat Rev Microbiol 15:271-284.
3. Yin W, Cai X, Ma H, Zhu L, Zhang Y, Chou S-H, Galperin MY, He J. 2020. A decade of research on the second messenger c-di-AMP. FEMS Microbiol Rev 44:701-724.
4. Irving SE, Choudhury NR, Corrigan RM. 2021. The stringent response and physiological roles of (pp)pGpp in bacteria. Nature Rev Microbiol 19:256-271.
5. Yoon SH, Waters CM. 2021. The ever-expanding world of bacterial cyclic oligonucleotide second messengers. Curr Opin Microbiol 60:96-103.
6. Hengge R. 2020. Linking bacterial growth, survival, and multicellularity – small signaling molecules as triggers and drivers. Curr Opin Microbiol 55:57-66.
7. Qi Y, Chuah ML, Dong X, Xie K, Luo Z, Tang K, Liang ZX. 2011. Binding of cyclic diguanylate in the non-catalytic EAL domain of FimX induces a long-range conformational change. J Biol Chem 286:2910-7.
8. Petters T, Zhang X, Nesper J, Treuner-Lange A, Gomez-Santos N, Hoppert M, Jenal U, Søgaard-Andersen L. 2012. The orphan histidine protein kinase SgmT is a c-di-GMP receptor and regulates composition of the extracellular matrix together with the orphan DNA binding response regulator DigR in *Myxococcus xanthus*. Mol Microbiol 84:147-65.
9. Newell PD, Boyd CD, Sondermann H, O'Toole GA. 2011. A c-di-GMP effector system controls cell adhesion by inside-out signaling and surface protein cleavage. PLoS Biol 9:e1000587.
10. Duerig A, Abel S, Folcher M, Nicollier M, Schwede T, Amiot N, Giese B, Jenal U. 2009. Second messenger-mediated spatiotemporal control of protein degradation regulates bacterial cell cycle progression. Genes Dev 23:93-104.
11. Navarro MVAS, De N, Bae N, Wang Q, Sondermann H. 2009. Structural analysis of the GGDEF-EAL domain-containing c-di-GMP receptor FimX. Structure 17:1104-1116.
12. Amikam D, Galperin MY. 2006. PilZ domain is part of the bacterial c-di-GMP binding protein. Bioinformatics 22:3-6.
13. Ryjenkov DA, Simm R, Römling U, Gomelsky M. 2006. The PilZ domain is a receptor for the second messenger c-di-GMP: the PilZ domain protein YcgR controls motility in enterobacteria. J Biol Chem 281:30310-4.
14. Ramelot TA, Yee A, Cort JR, Semesi A, Arrowsmith CH, Kennedy MA. 2007. NMR structure and binding studies confirm that PA4608 from *Pseudomonas aeruginosa* is a PilZ domain and a c-di-GMP binding protein. Proteins 66:266-71.
15. Christen M, Christen B, Allan MG, Folcher M, Jeno P, Grzesiek S, Jenal U. 2007. DgrA is a member of a new family of cyclic diguanosine monophosphate receptors and controls flagellar motor function in *Caulobacter crescentus*. Proc Natl Acad Sci U S A 104:4112-7.
16. Pratt JT, Tamayo R, Tischler AD, Camilli A. 2007. PilZ domain proteins bind cyclic diguanylate and regulate diverse processes in *Vibrio cholerae*. J Biol Chem 282:12860-70.
17. Wang YC, Chin KH, Tu ZL, He J, Jones CJ, Sanchez DZ, Yildiz FH, Galperin MY, Chou SH. 2016. Nucleotide binding by the widespread high-affinity cyclic di-GMP receptor MshEN domain. Nat Commun 7:12481.
18. Roelofs KG, Jones CJ, Helman SR, Shang X, Orr MW, Goodson JR, Galperin MY, Yildiz FH, Lee VT. 2015. Systematic identification of cyclic-di-GMP binding proteins in *Vibrio cholerae* reveals a novel class of cyclic-di-GMP-binding ATPases associated with type II secretion systems. PLoS Pathog 11:e1005232.

19. Tschowri N, Schumacher MA, Schlimpert S, Chinnam NB, Findlay KC, Brennan RG, Buttner MJ. 2014. Tetrameric c-di-GMP mediates effective transcription factor dimerization to control *Streptomyces* development. Cell 158:1136-1147.
20. Li W, He ZG. 2012. LtmA, a novel cyclic di-GMP-responsive activator, broadly regulates the expression of lipid transport and metabolism genes in *Mycobacterium smegmatis*. Nucl Acids Res 40:11292-307.
21. Fazli M, O'Connell A, Nilsson M, Niehaus K, Dow JM, Givskov M, Ryan RP, Tolker-Nielsen T. 2011. The CRP/FNR family protein Bcam1349 is a c-di-GMP effector that regulates biofilm formation in the respiratory pathogen *Burkholderia cenocepacia*. Mol Microbiol 82:327-41.
22. Chin KH, Lee YC, Tu ZL, Chen CH, Tseng YH, Yang JM, Ryan RP, McCarthy Y, Dow JM, Wang AH, Chou SH. 2010. The cAMP receptor-like protein CLP is a novel c-di-GMP receptor linking cell-cell signaling to virulence gene expression in *Xanthomonas campestris*. J Mol Biol 396:646-62.
23. Hickman JW, Harwood CS. 2008. Identification of FleQ from *Pseudomonas aeruginosa* as a c-di-GMP-responsive transcription factor. Mol Microbiol 69:376-89.
24. Krasteva PV, Fong JC, Shikuma NJ, Beyhan S, Navarro MV, Yildiz FH, Sondermann H. 2010. *Vibrio cholerae* VpsT regulates matrix production and motility by directly sensing cyclic di-GMP. Science 327:866-8.
25. Srivastava D, Harris RC, Waters CM. 2011. Integration of cyclic di-GMP and quorum sensing in the control of *vpsT* and *aphA* in *Vibrio cholerae*. J Bacteriol 193:6331-41.
26. Schäper S, Steinchen W, Krol E, Altegoer F, Skotnicka D, Søgaard-Andersen L, Bange G, Becker A. 2017. AraC-like transcriptional activator CuxR binds c-di-GMP by a PilZ-like mechanism to regulate extracellular polysaccharide production. Proc Natl Acad Sci USA 114:E4822-E4831.
27. Galperin MY, Chou SH. 2020. Structural conservation and diversity of PilZ-related domains. J Bacteriol 202.
28. Hengge R. 2009. Principles of c-di-GMP signalling in bacteria. Nat Rev Microbiol 7:263-73.
29. Hengge R. 2021. High-specificity local and global c-di-GMP signaling. Trends Microbiol doi:10.1016/j.tim.2021.02.003.
30. Munoz-Dorado J, Marcos-Torres FJ, Garcia-Bravo E, Moraleda-Munoz A, Perez J. 2016. Myxobacteria: Moving, killing, feeding, and surviving together. Front Microbiol 7:781.
31. Schumacher D, Søgaard-Andersen L. 2017. Regulation of cell polarity in motility and cell division in *Myxococcus xanthus*. Annu Rev Microbiol 71:61-78.
32. Zhang Y, Ducret A, Shaevitz J, Mignot T. 2012. From individual cell motility to collective behaviors: insights from a prokaryote, *Myxococcus xanthus*. FEMS Microbiol Rev 36:149-164.
33. Lee B, Holkenbrink C, Treuner-Lange A, Higgs PI. 2012. *Myxococcus xanthus* developmental cell fate production: heterogeneous accumulation of developmental regulatory proteins and reexamination of the role of MazF in developmental lysis. J Bacteriol 194:3058-68.
34. O'Connor KA, Zusman DR. 1991. Development in *Myxococcus xanthus* involves differentiation into two cell types, peripheral rods and spores. J Bacteriol 173:3318-33.
35. Wireman JW, Dworkin M. 1977. Developmentally induced autolysis during fruiting body formation by *Myxococcus xanthus*. J Bacteriol 129:798-802.
36. Kuzmich S, Skotnicka D, Szadkowski D, Klos P, Perez-Burgos M, Schander E, Schumacher D, Søgaard-Andersen L. 2021. Three PilZ domain proteins, PlpA, PixA and PixB, have distinct functions in regulation of motility and development in *Myxococcus xanthus*. J Bacteriol doi:10.1128/JB.00126-21.

37. Skotnicka D, Petters, T., Heering J, Hoppert M, Kaever V, Søgaard-Andersen L. 2016. Cyclic di-GMP regulates type IV pilus-dependent motility in *Myxococcus xanthus*. J Bacteriol 198:77-90.
38. Harris BZ, Kaiser D, Singer M. 1998. The guanosine nucleotide (p)ppGpp initiates development and A-factor production in *Myxococcus xanthus*. Genes Dev 12:1022-35.
39. Singer M, Kaiser D. 1995. Ectopic production of guanosine penta- and tetraphosphate can initiate early developmental gene expression in *Myxococcus xanthus*. Genes Dev 9:1633-44.
40. Skotnicka D, Smaldone GT, Petters T, Trampari E, Liang J, Kaever V, Malone JG, Singer M, Søgaard-Andersen L. 2016. A minimal threshold of c-di-GMP is essential for fruiting body formation and sporulation in *Myxococcus xanthus*. PLoS Genet 12:e1006080.
41. Kroos L. 2017. Highly signal-responsive gene regulatory network governing *Myxococcus* development. Trends Genet 33:3-15.
42. Konovalova A, Petters T, Sogaard-Andersen L. 2010. Extracellular biology of Myxococcus xanthus. FEMS Microbiol Rev 34:89-106.
43. Sun H, Shi W. 2001. Genetic studies of *mrp*, a locus essential for cellular aggregation and sporulation of *Myxococcus xanthus*. J Bacteriol 183:4786-95.
44. McLaughlin PT, Bhardwaj V, Feeley BE, Higgs PI. 2018. MrpC, a CRP/Fnr homolog, functions as a negative autoregulator during the *Myxococcus xanthus* multicellular developmental program. Mol Microbiol 109:245-261.
45. Ueki T, Inouye S. 2003. Identification of an activator protein required for the induction of *fruA*, a gene essential for fruiting body development in *Myxococcus xanthus*. Proc Natl Acad Sci U S A 100:8782-8787.
46. Lee J-s, Son B, Viswanathan P, Luethy PM, Kroos L. 2011. Combinatorial regulation of *fmgD* by MrpC2 and FruA during *Myxococcus xanthus* development. J Bacteriol 193:1681-1689.
47. Mittal S, Kroos L. 2009. A combination of unusual transcription factors binds cooperatively to control *Myxococcus xanthus* developmental gene expression. Proc Natl Acad Sci U S A 106:1965-1970.
48. Son B, Liu Y, Kroos L. 2011. Combinatorial regulation by MrpC2 and FruA involves three sites in the *fmgE* promoter region during *Myxococcus xanthus* development. J Bacteriol 193:2756-2766.
49. Campbell A, Viswanathan P, Barrett T, Son B, Saha S, Kroos L. 2015. Combinatorial regulation of the *dev* operon by MrpC2 and FruA during *Myxococcus xanthus* development. J Bacteriol 197:240-51.
50. Robinson M, Son B, Kroos D, Kroos L. 2014. Transcription factor MrpC binds to promoter regions of hundreds of developmentally-regulated genes in *Myxococcus xanthus*. BMC Genomics 15:1123.
51. Mittal S, Kroos L. 2009. Combinatorial regulation by a novel arrangement of FruA and MrpC2 transcriptionfactors during *Myxococcus xanthus* development. J Bacteriol 191:2753-2763.
52. Ellehauge E, Nørregaard-Madsen M, Søgaard-Andersen L. 1998. The FruA signal transduction protein provides a checkpoint for the temporal co-ordination of intercellular signals in *Myxococcus xanthus* development. Mol Microbiol 30:807-17.
53. Ogawa M, Fujitani S, Mao X, Inouye S, Komano T. 1996. FruA, a putative transcription factor essential for the development of *Myxococcus xanthus*. Mol Microbiol 22:757-67.
54. Wright TA, Jiang L, Park JJ, Anderson WA, Chen G, Hallberg ZF, Nan B, Hammond MC. 2020. Second messengers and divergent HD-GYP phosphodiesterases regulate 3',3'-cGAMP signaling. Mol Microbiol 113:222-236.

55. Lancero H, Caberoy NB, Castaneda S, Li Y, Lu A, Dutton D, Duan XY, Kaplan HB, Shi W, Garza AG. 2004. Characterization of a *Myxococcus xanthus* mutant that is defective for adventurous motility and social motility. Microbiology 150:4085-93.
56. Caberoy NB, Welch RD, Jakobsen JS, Slater SC, Garza AG. 2003. Global mutational analysis of NtrC-like activators in *Myxococcus xanthus*: Identifying activator mutants defective for motility and fruiting body development. J Bacteriol 185:6083-6094.
57. Skotnicka D, Steinchen W, Szadkowski D, Cadby IT, Lovering AL, Bange G, Søgaard-Andersen L. 2020. CdbA is a DNA-binding protein and c-di-GMP receptor important for nucleoid organization and segregation in *Myxococcus xanthus*. Nat Commun 11:1791.
58. Guzzo CR, Salinas RK, Andrade MO, Farah CS. 2009. PilZ protein structure and interactions with PilB and the FimX EAL domain: Implications for control of type IV pilus biogenesis. J Mol Biol 393:848-866.
59. Munoz-Dorado J, Inouye S, Inouye M. 1991. A gene encoding a protein serine/threonine kinase is required for normal development of *M. xanthus*, a gram-negative bacterium. Cell 67:995-1006.
60. Jakovljevic V, Leonardy S, Hoppert M, Søgaard-Andersen L. 2008. PilB and PilT are ATPases acting antagonistically in type IV pili function in *Myxococcus xanthus*. J Bacteriol 190:2411-2421.
61. Pogue CB, Zhou T, Nan B. 2018. PlpA, a PilZ-like protein, regulates directed motility of the bacterium *Myxococcus xanthus*. Mol Microbiol 107:214-228.
62. Ettwiller L, Buswell J, Yigit E, Schildkraut I. 2016. A novel enrichment strategy reveals unprecedented number of novel transcription start sites at single base resolution in a model prokaryote and the gut microbiome. BMC Genomics 17:199.
63. Nariya H, Inouye S. 2005. Identification of a protein Ser/Thr kinase cascade that regulates essential transcriptional activators in *Myxococcus xanthus* development. Mol Microbiol 58:367-379.
64. Nariya H, Inouye S. 2006. A protein Ser/Thr kinase cascade negatively regulates the DNA-binding activity of MrpC, a smaller form of which may be necessary for the *Myxococcus xanthus* development. Mol Microbiol 60:1205-1217.
65. Lee B, Mann P, Grover V, Treuner-Lange A, Kahnt J, Higgs PI. 2011. The *Myxococcus xanthus* spore cuticula protein C is a fragment of FibA, an extracellular metalloprotease produced exclusively in aggregated cells. PLoS One 6:e28968.
66. Savery N, Rhodius V, Busby SJW, Busby SJW, Grosveld FG, Latchman DS. 1996. Protein-protein interactions during transcription activation: the case of the *Escherichia coli* cyclic AMP receptor protein. Philos Trans R Soc Lond B Biol Sci 351:543-550.
67. Richet E, Søgaard-Andersen L. 1994. CRP induces the repositioning of MalT at the *Escherichia coli malK*p promoter primarily through DNA bending. EMBO J 13:4558-4567.
68. Müller F-D, Treuner-Lange A, Heider J, Huntley S, Higgs P. 2010. Global transcriptome analysis of spore formation in *Myxococcus xanthus* reveals a locus necessary for cell differentiation. BMC Genomics 11:264.
69. Hallberg ZF, Wang XC, Wright TA, Nan B, Ad O, Yeo J, Hammond MC. 2016. Hybrid promiscuous (Hypr) GGDEF enzymes produce cyclic AMP-GMP (3', 3'-cGAMP). Proc Natl Acad Sci U S A 113:1790-1795.
70. Lori C, Ozaki S, Steiner S, Böhm R, Abel S, Dubey BN, Schirmer T, Hiller S, Jenal U. 2015. Cyclic di-GMP acts as a cell cycle oscillator to drive chromosome replication. Nature 523:236-239.
71. Kaiser D. 1979. Social gliding is correlated with the presence of pili in *Myxococcus xanthus*. Proc Natl Acad Sci USA 76:5952-5956.
72. Shi X, Wegener-Feldbrügge S, Huntley S, Hamann N, Hedderich R, Søgaard-Andersen L. 2008. Bioinformatics and experimental analysis of proteins of two-component systems in *Myxococcus xanthus*. J Bacteriol 190:613-624.

73. Hodgkin J, Kaiser D. 1977. Cell-to-cell stimulation of movement in nonmotile mutants of *Myxococcus*. Proc Natl Acad Sci U S A 74:2938-42.
74. Sambrook J, Russell DW. 2001. Molecular cloning : a laboratory manual, 3rd ed. Cold Spring Harbor Laboratory Press, Cold Spring Harbor, N.Y.
75. Langmead B, Salzberg SL. 2012. Fast gapped-read alignment with Bowtie 2. Nat Methods 9:357-9.
76. Li H, Handsaker B, Wysoker A, Fennell T, Ruan J, Homer N, Marth G, Abecasis G, Durbin R, Genome Project Data Processing S. 2009. The Sequence Alignment/Map format and SAMtools. Bioinformatics 25:2078-9.
77. Liao Y, Smyth GK, Shi W. 2014. featureCounts: an efficient general purpose program for assigning sequence reads to genomic features. Bioinformatics 30:923-30.
78. Liao Y, Smyth GK, Shi W. 2019. The R package Rsubread is easier, faster, cheaper and better for alignment and quantification of RNA sequencing reads. Nucleic Acids Res 47:e47.
79. Love MI, Huber W, Anders S. 2014. Moderated estimation of fold change and dispersion for RNA-seq data with DESeq2. Genome Biol 15:550.
80. McCleary WR, Esmon B, Zusman DR. 1991. *Myxococcus xanthus* protein C is a major spore surface protein. J Bacteriol 173:2141-5.
81. Bulyha I, Schmidt C, Lenz P, Jakovljevic V, Hone A, Maier B, Hoppert M, Sogaard-Andersen L. 2009. Regulation of the type IV pili molecular machine by dynamic localization of two motor proteins. Mol Microbiol 74:691-706.
82. Schindelin J, Arganda-Carreras I, Frise E, Kaynig V, Longair M, Pietzsch T, Preibisch S, Rueden C, Saalfeld S, Schmid B, Tinevez JY, White DJ, Hartenstein V, Eliceiri K, Tomancak P, Cardona A. 2012. Fiji: an open-source platform for biological-image analysis. Nat Methods 9:676-82.
83. Yoder-Himes DR, Kroos L. 2006. Regulation of the *Myxococcus xanthus* C-signal-dependent Omega4400 promoter by the essential developmental protein FruA. J Bacteriol 188:5167-76.
84. Finn RD, Coggill P, Eberhardt RY, Eddy SR, Mistry J, Mitchell AL, Potter SC, Punta M, Qureshi M, Sangrador-Vegas A, Salazar GA, Tate J, Bateman A. 2016. The Pfam protein families database: towards a more sustainable future. Nucl Acids Res 44:D279-85.
85. Almagro Armenteros JJ, Tsirigos KD, Sonderby CK, Petersen TN, Winther O, Brunak S, von Heijne G, Nielsen H. 2019. SignalP 5.0 improves signal peptide predictions using deep neural networks. Nat Biotechnol 37:420-423.
86. Julien B, Kaiser AD, Garza A. 2000. Spatial control of cell differentiation in *Myxococcus xanthus*. Proc Natl Acad Sci USA 97:9098-103.
87. Wu SS, Kaiser D. 1997. Regulation of expression of the *pilA* gene in *Myxococcus xanthus*. J Bacteriol 179:7748-7758.

970 **Table 1.** *M. xanthus* strains used in this study

| Strain | Characteristics | Reference |
|---|---|---|
| DK1622 | Wild-type (WT) | (71) |
| SA5605 | Δ*dmxB* | (37) |
| SA3546 | Δ*pmxA* | (37) |
| SA6462 | Δ*mrpC* | (36) |
| SA8038 | *pmxA*::*pmxA*-mVenus | This study |
| SA8044 | Δ*mrpC, pmxA*::*pmxA-mVenus* | This study |
| SA8096 | *attB*::pSK65 (mCherry) | This study |
| SA8098 | *attB*::pSK81 ($P_{pmxA}$-mCherry) | This study |
| SA10108 | *attB*::pSK103 ($P_{pmxA}^{BS1*}$-mCherry) | This study |
| SA10109 | *attB*::pSK105 ($P_{pmxA}^{BS2*}$-mCherry) | This study |
| SA10111 | *attB*::pSK111 ($P_{pmxA}^{BS1*/BS2*}$-mCherry) | This study |
| SA8099 | *attB*::pSK101 ($P_{dmxB}$-mCherry) | This study |
| SA10110 | *attB*::pSK112 ($P_{dmxB}^{BS4*}$-mCherry) | This study |
| SA10133 | Δ*dmxB* Δ*mrpC* | This study |
| SA10113 | Δ*mrpC attB*::pSK81 ($P_{pmxA}$-mCherry) | This study |
| SA10105 | Δ*mrpC attB*::pSK101 ($P_{dmxB}$-mCherry) | This study |
| SA8037 | Δ*pmxA* Δ*mrpC* | This study |

971

972

973 **Table 2.** Plasmids used in this study

| Plasmid | Description | Reference |
|---|---|---|
| pBJ114 | *galK*, $Kan^R$ | (86) |
| pSWU30 | *attP*, $Tet^R$ | (87) |
| pPH158 | pET28a(+), $His_6$-*mrpC*, $Kan^R$ | (33) |
| pSK29 | pBJ114, *pmxA*-mVenus, gene replacement at native site, $Kan^R$ | This study |
| pSK65 | pSWU30, mCherry, *attB*, $Tc^R$ | This study |
| pSK81 | pSWU30, $P_{pmxA}$-mCherry, *attB*, $Tc^R$ | This study |
| pSK103 | pSWU30, $P_{pmxA}^{BS1*}$-mCherry, *attB*, $Tc^R$ | This study |
| pSK105 | pSWU30, $P_{pmxA}^{BS2*}$-mCherry, *attB*, $Tc^R$ | This study |
| pSK114 | pSWU30, $P_{pmxA}^{BS3}$-mCherry, *attB*, $Tc^R$ | This study |
| pSK111 | pSWU30, $P_{pmxA}^{BS1*/BS2*}$-mCherry, *attB*, $Tc^R$ | This study |
| pSK101 | pSWU30, $P_{dmxB}$-mCherry, *attB*, $Tc^R$ | This study |
| pSK121 | pSWU30, $P_{dmxB}^{BS1*}$-mCherry, *attB*, $Tc^R$ | This study |
| pSK115 | pSWU30, $P_{dmxB}^{BS2*}$-mCherry, *attB*, $Tc^R$ | This study |
| pSK109 | pSWU30, $P_{dmxB}^{BS3*}$-mCherry, *attB*, $Tc^R$ | This study |
| pSK112 | pSWU30, $P_{dmxB}^{BS4*}$-mCherry, *attB*, $Tc^R$ | This study |

974

975

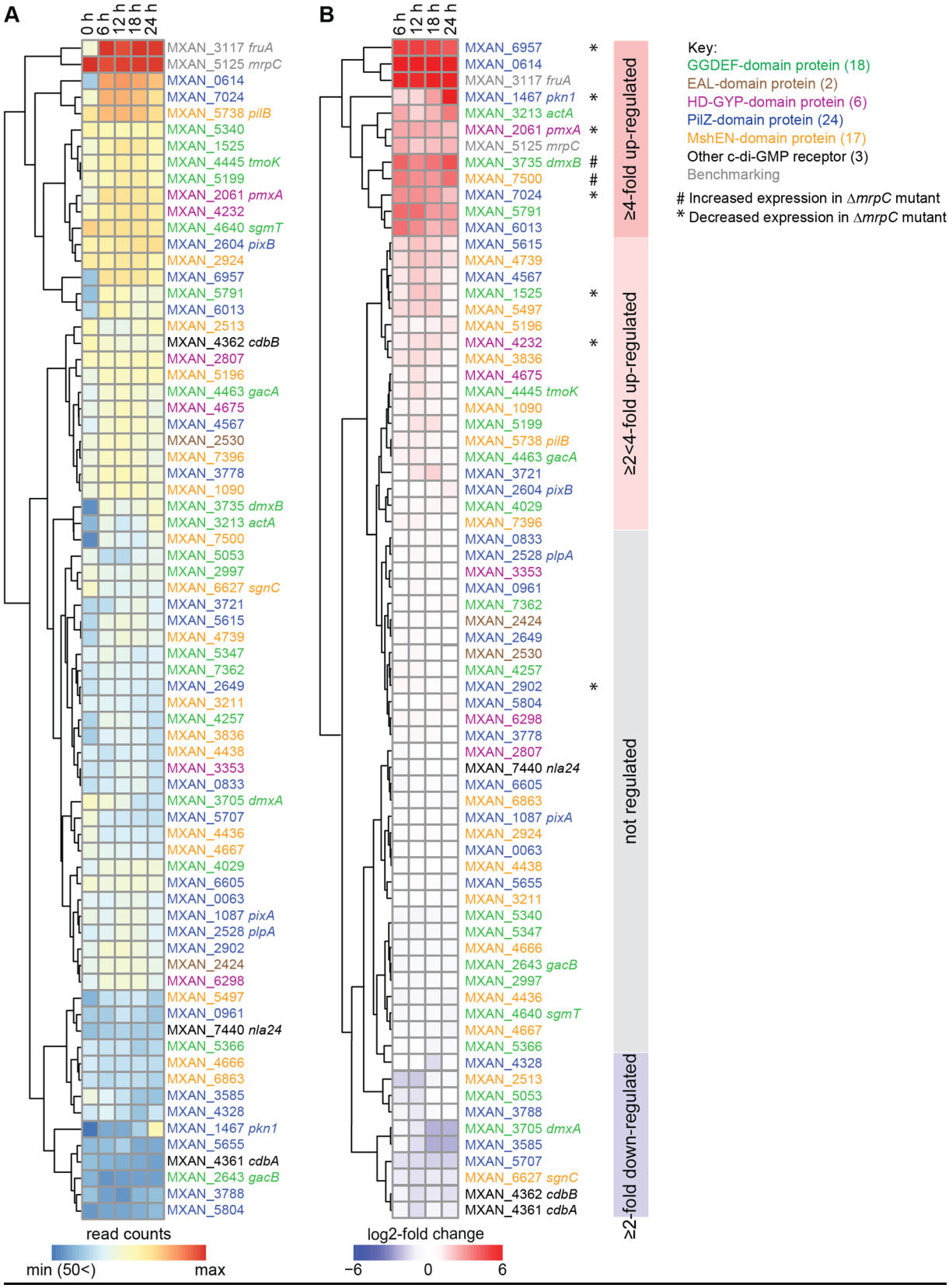

Figure 1. Expression of genes for “c-di-GMP associated proteins”

A. Expression of the genes encoding “c-di-GMP associated proteins”. Heat-map represents normalized read counts at the indicated time points. Genes are colour-coded according to the key on the right. MXAN_2807 is indicated as a protein with an HD-GYP domain; this protein also contains a MshEN domain.

B. Relative transcript levels during development for genes encoding “c-di-GMP associated proteins”. Heat-map indicates log2-fold change at 6, 12, 18 or 24 h of development compared to 0 h. Genes marked * or # were expressed at lower and higher levels, respectively in the Δ*mrpC* mutant compared to WT as determined using RT-qPCR (See also Fig. 2 and Fig. S3). Coloured boxed on the right indicate the four clusters with distinct expression profiles.

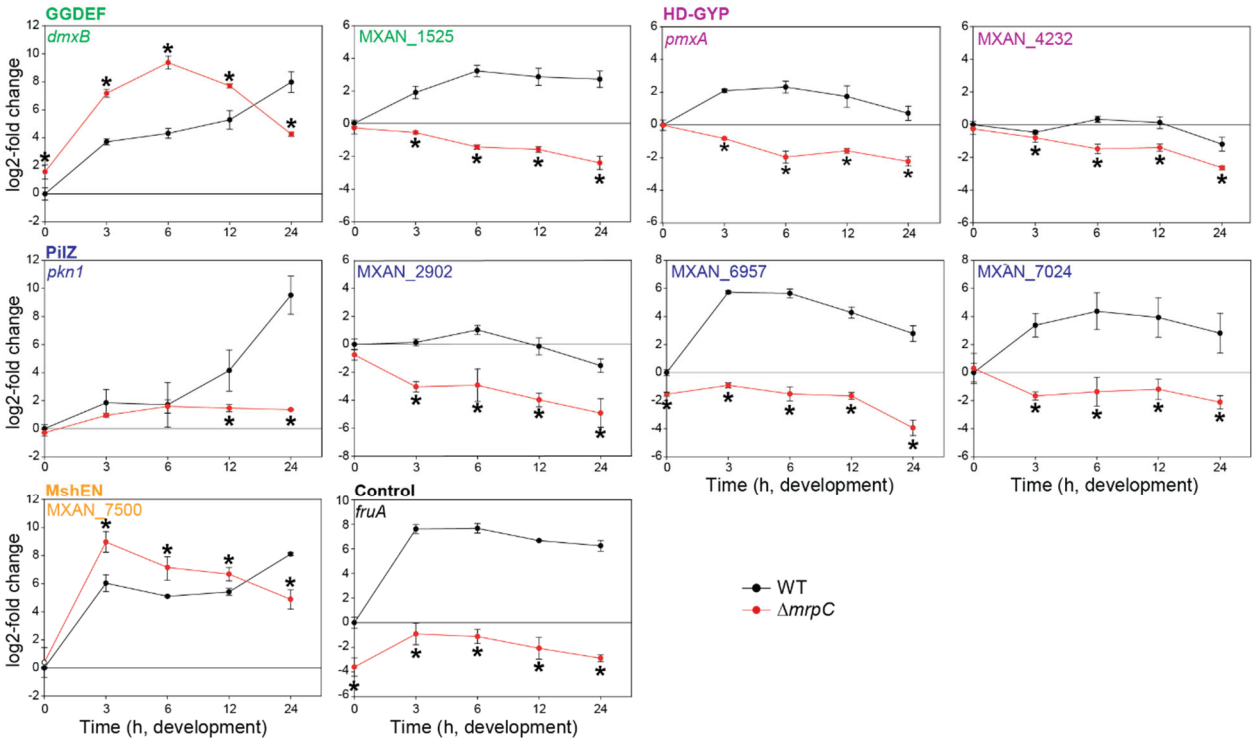


Figure 2. Regulation of expression of genes encoding "c-di-GMP associated proteins" by MrpC. Total RNA was isolated from cells developed in MC7 submerged cultures at the indicated time points from WT (black) and the Δ*mrpC* mutant (red). Transcript levels are shown as mean ± standard deviation (SD) from two biological replicates, each with two technical replicate, relative to WT at 0 h. *, *P*-value <0.05 in Student's t-test in which samples from the Δ*mrpC* mutant were compared to the samples from WT at the same time point. *fruA* served as a positive control. Based on protein sequence analysis, MXAN_1525 and MXAN_4232 are predicted to have DGC and PDE activity, respectively; however, neither a ΔMXAN_1525 nor a ΔMXAN_4232 mutant has defects during growth or development (37, 40). *pkn1,* MXAN_2902, MXAN_6957 and MXAN_7024 are PilZ-domain proteins; however, none contain the conserved motifs for c-di-GMP binding (27, 36). Except for Pkn1, lack of any of these four proteins does not cause defects during growth or development (36, 59). MXAN_7500 is a MshEN-domain protein with the sequence motifs for c-di-GMP binding (17); however, it is known not whether this protein binds c-di-GMP or whether it is important during growth and development.

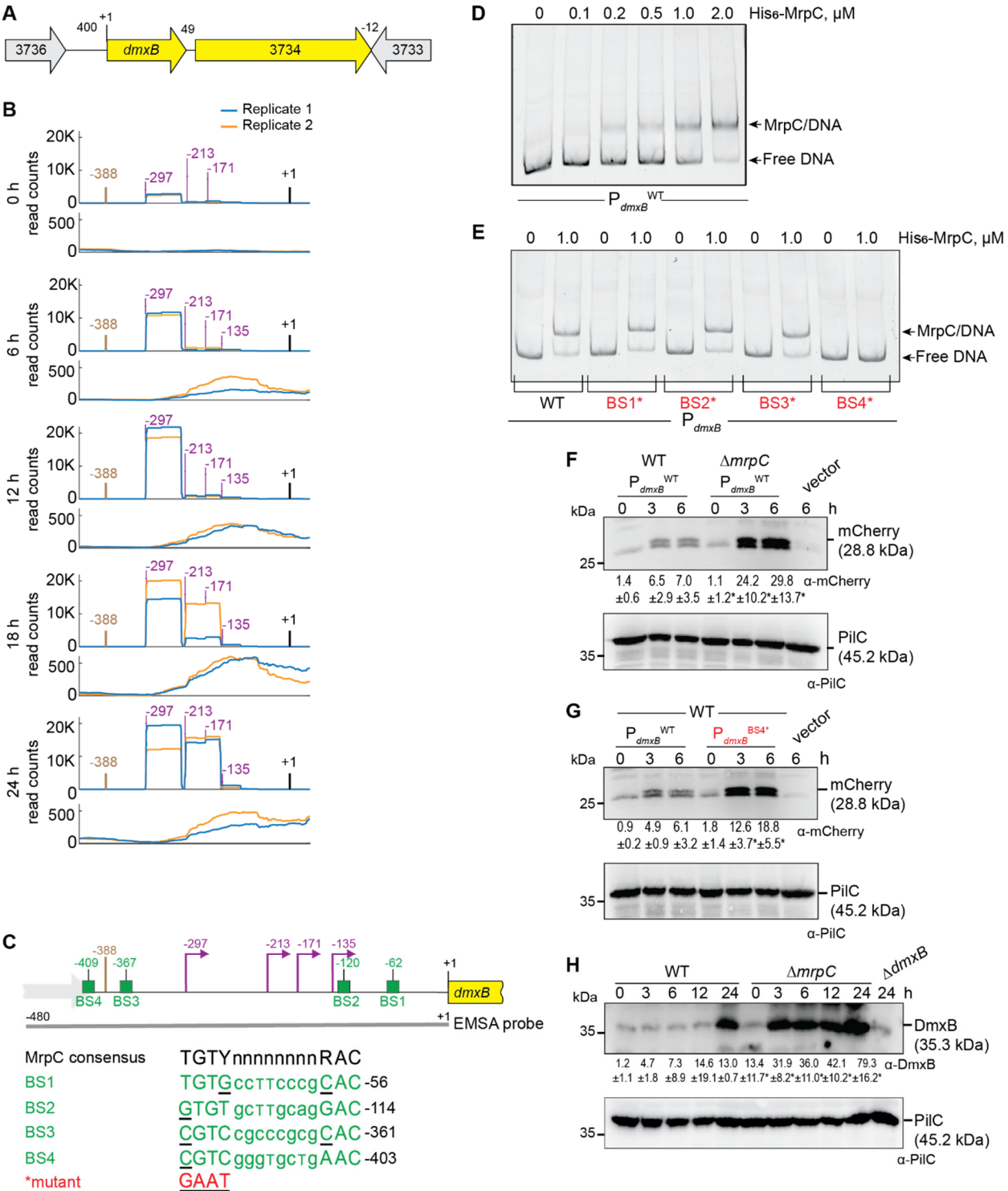


Figure 3. MrpC negatively regulates expression of *dmxB*

A. Schematic of *dmxB* locus. Direction of transcription is indicated by the arrows. +1 indicates TSC of *dmxB*. Numbers above indicate distance between start and stop codons of flanking genes. MXAN_3734 encodes a response regulator that is not important for development (40).

B. Visualization of RNA-seq (lower panels) and Cappable-seq (upper panels) data at different time points. For each time point, mapped read counts for both biological replicates are shown in blue and orange. Data from RNA-seq and Cappable-seq are from different samples. +1 indicates the *dmxB* TSC. TSSs as mapped by Cappable-seq are indicated in purple relative to the TSC of *dmxB*. The center of the MrpC ChIP-seq peak is in brown.

C. Feature map of *dmxB* promoter region. +1 and colour code is as in B. Green boxes labelled BS1-4 indicate potential MrpC binding sites based on the consensus sequence as defined by (50); sequences of BS1-4 are shown below and in which underlining indicate a mismatch. Red indicates the sequence used to generate the mutant binding sites.

D, E. MrpC binds to the *dmxB* promoter region using BS4. The indicated Hex-labelled probes were mixed with the indicated concentrations of $His_6$-MrpC EMSA and analyzed by EMSA.

F. MrpC represses *dmxB* promoter(s). Total cell lysates from the indicated strains expressing *mcherry* from $P_{dmxB}^{WT}$ were harvested from cells developed in MC7 submerged cultures at the indicated time points. 10 µg of protein were loaded per lane and samples separated by SDS-PAGE. Upper and lower blots were probed with α-mCherry and α-PilC antibodies, respectively. PilC blot served as loading control. Numbers below upper panel indicate in the accumulation of mCherry relative to PilC as mean ± SD as measured in three biological replicates. *, *P*-value <0.05 in Student's t-test in which samples from the Δ*mrpC* mutant were compared to samples from WT at the same time point. Vector with *mCherry* but without the *dmxB* promoter served as a negative control (vector). mCherry separates into two bands; the reason for this is not known.

G. BS4 is important for MrpC-dependent repression of *dmxB* promoter(s). Total cell lysates from the indicated WT strains expressing mCherry from the two indicated promoters were prepared and analyzed as in F.

H. DmxB accumulates at increased levels in the Δ*mrpC* mutant. Total cell lysates of the indicated strains were harvested from cells developed in MC7 submerged conditions at indicated time points and analyzed as in F.

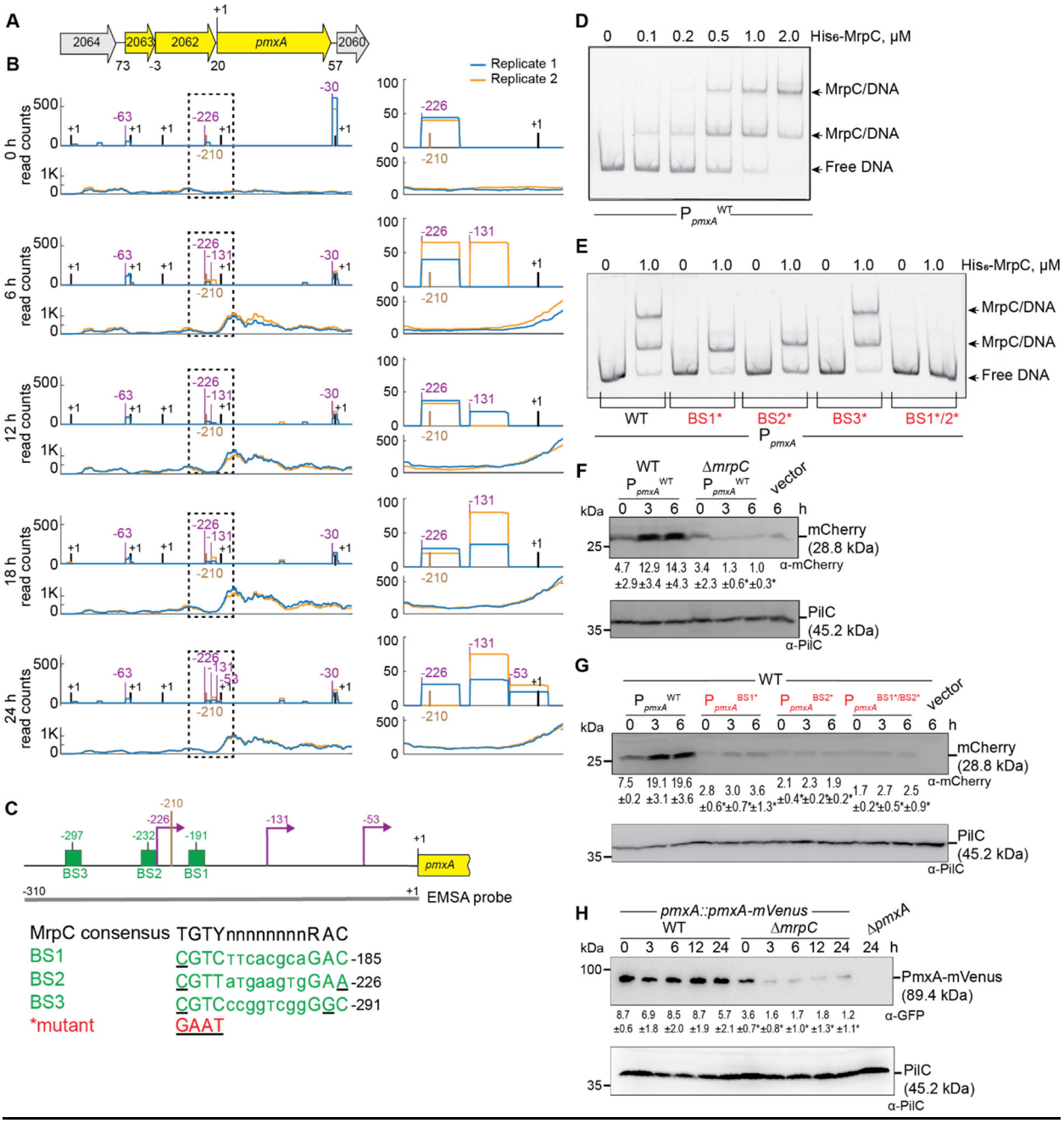


1039

1040 Figure 4. MrpC positively regulates expression of *pmxA*.

1041 A. Schematic of *pmxA* locus. Direction of transcription is indicated by the arrows. +1 indicates
1042 TSC of *pmxA*. Numbers above indicate distance between start and stop codons of flanking
1043 genes. MXAN_2063 encodes a FecR domain-containing protein with a lipoprotein signal peptide
1044 and MXAN_2062 encodes a protein with a type I signal peptide, an N-terminal LysM domain
1045 and a C-terminal extracellular fibronectin type III domain. The function of these two proteins is
1046 not known.

B. Visualization of RNA-seq (lower panels) and Cappable-seq (upper panels) data at different time points for genes at *pmxA* locus. For each time point, mapped read counts for both biological replicates are shown in blue and orange. The data from RNA-seq and Cappable-seq were obtained from different samples. Left panels, +1 indicates TSCs of MXAN_2064-_2060; right panels, zoom of region indicated in the hatched box in left panels immediately upstream of *pmxA* and where +1 indicates the TSC of *pmxA*. In both sets of panels, TSSs as mapped by Cappable-seq are indicated in purple relative to the nearest TSC. The center of the MrpC ChIP-seq peak is in brown.

C. Feature map of *pmxA* promoter region. +1 and colour code is as in B. Green boxes labelled BS1-3 indicate potential MrpC binding sites based on the consensus sequence as defined by (50); sequences of BS1-3 are shown below and in which underlining indicate a mismatch. Red indicates the sequence used to generate the mutant binding sites.

D, E. MrpC binds to the *pmxA* promoter region using BS1 and BS2. The indicated Hex-labelled probes were mixed with the indicated concentrations of $His_6$-MrpC EMSA and analyzed by EMSA.

F. MrpC activates *pmxA* promoter(s). Total cell lysates from the indicated strains expressing *mcherry* from $P_{pmxA}^{WT}$ were harvested from cells developed in MC7 submerged cultures at the indicated time points and then analyzed as in Fig. 3F.

G. BS1 and BS2 are important for MrpC-dependent activation of the *pmxA* promoter(s). Total cell lysates from the indicated WT strains expressing mCherry from the indicated promoters were prepared and analyzed as in Fig. 3F.

H. PmxA accumulates at reduced levels in the Δ*mrpC* mutant. Total cell lysates of the indicated strains were harvested from cells developed in MC7 submerged conditions at indicated time points and analyzed as in Fig. 3F.

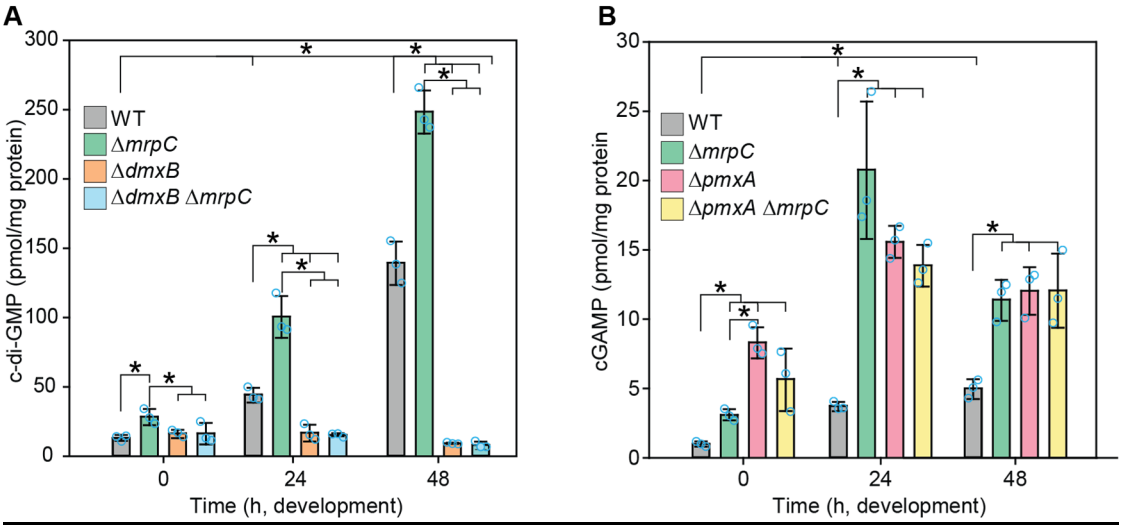


Figure 5. c-di-GMP and cGAMP accumulation in WT and Δ*mrpC* mutant during development.

A, B. c-di-GMP and cGAMP levels during growth and development. Cells were harvested at the indicated time points of development, and nucleotide levels and protein concentrations determined. Levels are shown as mean±SD calculated from three biological replicates. Individual data points are in light blue. *, *P*-value <0.05 in Student's t-test.

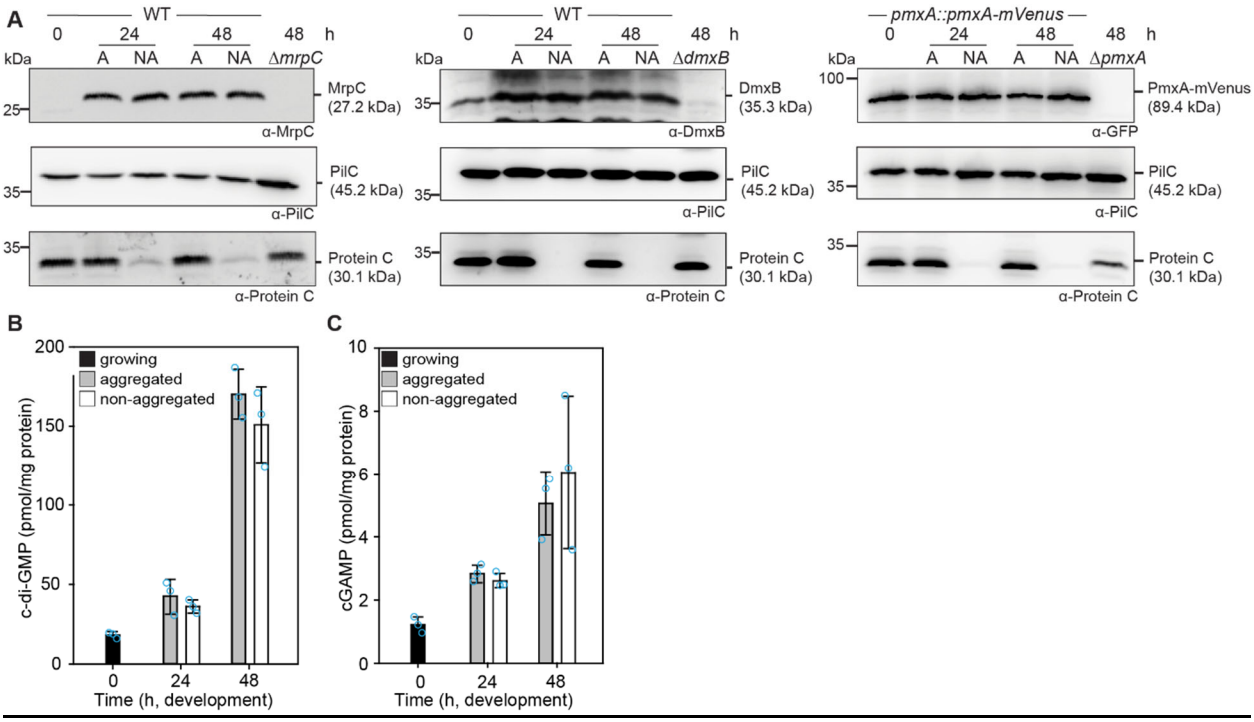


Figure 6. MrpC, DmxA, PmxA-mVenus, c-di-GMP and cGAMP accumulation in aggregated and non-aggregated cells.

A. MrpC, DmxB and PmxA-mVenus accumulate at the same levels in aggregated and non-aggregated cells. Cells were harvested at the indicated time points of development and separated into the two cell fractions. 10 µg of protein was loaded per lane and samples separated by SDS-PAGE. Upper blots were probed with α-MrpC, α-DmxB or α-GFP, middle blots with α-PilC, and lower blots with α-Protein C antibodies. The PilC blots served as loading controls and the Protein C blots as cell separation controls.

B, C. c-di-GMP (B) and cGAMP (C) accumulate at the same levels in aggregated and non-aggregated cells of WT. Samples were generated as in A. Levels are shown as mean±SD calculated from three biological replicates. Individual data points are in light blue. *, *P*-value <0.05 in Student's t-test.

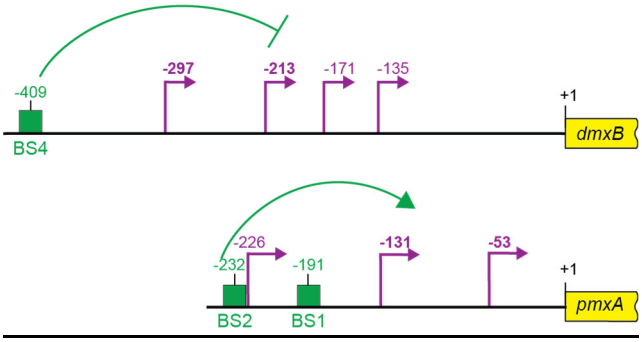


Figure 7. Schematic of *dmxB* and *pmxA* promoter regions.

+1 indicate TSC of *dmxB* or *pmxA*; potential TSSs are indicated in purple with developmentally regulated TSSs in bold; green boxes indicate verified MrpC binding sites named as in Fig. 3C and 4C. All coordinates are relative to the TSC (+1).